RHODES COLLEGE

Science Journal

Volume VII May 1989

Individual Research

The Rhodes College Science Journal

Volume VII
May 1989

Preface

The Rhodes College Science Journal is a student-edited annual publication which recognizes the scientific achievements of Rhodes students. Founded six years ago as a scholarly forum for student research and scientific ideas, the journal aims to maintain and stimulate the tradition of independent study. We hope that in reading the journal, other students will be encouraged to pursue scientific investigations and research.

Editors
Ken Cameron, William Holden, Anne Junkin

Staff
Barbara Mulach
Blaik Mathews
Steve Hipp
Lori Vallelunga
Leigh Robin
Margaret Pomphrey
John Swift

Acknowledgements
Dr. David Kesler
Dr. Harmon Dunathan
Alumni and friends
whose generosity
has helped make
this publication possible.

The Morphology of the Antarctic Ozone Hole vs. the Temperature Structure

Anne L. Junkin†

Abstract

Aikin and McPeters ["3-D Morphology of the Antarctic Ozone Hole," Geophysical Research Letters, May 1988] found that the springtime Antarctic Ozone hole exists at altitudes higher than where polar stratospheric clouds, accepted as the site for the heterogeneous chemistry that causes the hole, are found, meaning that another mechanism is at work at these upper altitudes (33-55 km). Thus, we examined the relationship between the springtime Antarctic ozone depletion and the structure of the polar vortex. We confirmed the existence of ozone depletion at high altitudes, with the following unusual features: in agreement with Aikin and McPeters [1988] we found that although the ozone did form a pole-centered minimum, it increased instead of decreased throughout October in layer 7-8 (33-43 km), and in layer 9-10 (43-55 km) there was an ozone depletion similar to layer 2-3-4 (10-24 km), but it was accompanied by an overall ozone reduction. From the temperature data, we found a correlation between the temperature and ozone behavior at each of the layers. Layers 2-3-4 and 9-10 had similar temperature structures, but gradients of opposite sign, and layer 7-8's temperature structure reflected the fact that it is a transition layer possibly explaining the unusual behavior of the ozone levels in layer 7-8.

Introduction

In the Southern Hemisphere's spring, an ozone hole has formed above Antarctica in association with the polar vortex since 1979 as Farman et al, [1985] found by analyzing ground based data and Stolarski et al [1986] confirmed using satellite data. Solomon et al [1986] and McElroy [1986] suggested that since at this same time and place, polar stratospheric clouds (PSC's) were present [Hamill et al, 1986], there is a relationship between PSC's and ozone depletion. The PSC evaporation in the spring is accompanied by increases in chlorine as found by in situ flights [Farmer, 1987] because PSC's provide the site for Cl release into the lower stratosphere allowing the Cl to catalytically reduce ozone amounts. Therefore, the Cl originally contained in chloroflourocarbons (CFC's) but released on the PSC's cause this ozone hole as the amount of CFC's in the atmosphere increases with the continuing production of them on Earth. If the ozone minimum were limited to the altitudes where PSC's exist, the theory would be fairly complete, but, from satellite data, Aikin and McPeters [1988] showed that ozone depletion also occurs in the upper stratosphere (33-55 km) in the absence of PSC's, indicating that another mechanism causes the ozone minimum there. Thus, we will examine the structure of the polar vortex that forms concurrently with the ozone depletion to determine the relationship between the two effects in hopes of finding a mechanism for

† Anne is a senior physics major from Due West, SC.

ozone reduction at upper altitudes.

First, we will look in more detail at the role of Cl and PSC's in ozone depletion in the lower stratosphere (10-33 km). Ozone amounts decrease as a result of reacting with a free oxygen atom and forming two oxygen molecules. Chlorine as a catalyst for this reaction as illustrated below:

$$Cl + O_3 \rightarrow ClO + O_2$$
$$ClO + O \rightarrow Cl + O_2$$
$$\text{----------}$$
$$O_3 + O \rightarrow 2O_2$$

With the increase in CFC's, there is an increase of chlorine in the stratosphere. CFC's are chemically non-reactive, so they do not react with anything in the troposphere; instead, they are transported up to the stratosphere where they absorb high energy ultraviolet rays which cause them to dissociate, releasing chlorine. Normally, most of this chlorine is stored in the form of HCl and ClONO2, called chlorine reservoirs, preventing the chlorine from destroying the ozone [Levi 1988].

However, in the Antarctic region during the winter the conditions causing the vortex and PSC formation results in heterogeneous chemistry. During the winter, there is a period of total darkness, polar night, and a polar wind vortex is formed. Within this vortex, PSCs form [McCormick et al, 1982] and provide the site for this heterogeneous chemistry. Turco et al [1988] proposes that HCl and ClNO2 are adsorbed on the PSC particles and dissociate yielding the following reaction

$$ClNO_3 + HCl \rightarrow Cl_2 + HNO_3(s)$$

when spring comes and the atmosphere begins to warm. The PSC's evaporate and as they do, HNO3(s) precipitates out. Chlorine leaves in the form of Cl2 as well as HOCl and ClNO2, all of which are reactive [Turco et al 1988]. These chlorine species become the catalysts for ozone depletion as described above so the O3 levels begin to decrease above the pole in the springtime. This theory involving PSC's in the polar vortex is not, however, useful in explaining ozone depletion at higher altitudes, because PSCs seem to be limited to lower layers in the atmosphere (10-25 km) [Solomon 1988].

The ozone depletion is limited to a region above the pole contained within the polar vortex because the calm center allows PSCs to form in the middle of the vortex. Since there is less thermal energy from the sun, and little vertical wave motion, the polar vortex forms. Without this energy and the accompanying forces, the remaining forces on the atmosphere to drive the winds are those due to the rotation of the Earth. Most of the energy in the atmosphere is in the troposphere, and vertical waves are the means for energy transport, bring this energy up to the upper atmosphere. When winds near the Earth's surface hit land, they send a vertical wave up into the atmosphere transporting energy up. The Northern Hemisphere, even though it has the polar night, does not have as string a vortex because it gets the energy transported up by vertical winds. However, since only a small percentage of the land on the globe is in the Southern Hemisphere, there is less land to cause these vertical winds. In absence of thermal energy and the energy transported from the troposphere, the forces are the Coriolis force and the other forces due to the rotation of the Earth, giving rise to the circular wind pattern over the Pole, or the polar vortex.

Procedure

In order to approximate the shape and size of the polar vortex at different altitudes for comparison with ozone data, we made ozone, geopotential and temperature contour plots for the Southern Hemisphere and analyzed this data. The ozone data we examined were gathered by the SBUV (Solar Backscatter Ultraviolet) instrument on Nimbus-7 satellite during the Southern Hemisphere's spring in 1985. Simplified, the SBUV instrument compares the ultraviolet light directly from the sun with UV light reflected off the atmosphere. The two UV photon pairs used are about 200 A apart, one with strong ozone absorption and the other with weak absorption [Heath et al 1973].

Using this data, we made contour plots (see fig. 2a-d) of the amount of ozone, measured in Dobson units (1 DU = vertical column amount of a 0.01mm thick layer of ozone at STP), for a given day and a given Umkehr layer. An Umkehr layer corresponds in the following way to pressure levels and altitude:

Table 1

Umkehr Layer	pressure	altitude
2-3-4	250-33 mBar	10-24 km
5-6	33-8	24-33
7-8	8-2	33-43
9-10	2-0.5	43-55

[table adapted from Appendix J of Atmospheric Ozone 1985]

Since SBUV measures in terms of pressure levels, the altitude relationship is appropriate.

The temperature and geopotential data are from the National Meterological Center. From these data, after writing appropriate computer programs, we made contour temperature and geopotential plots. However, the data set was obtained in terms of pressure levels instead of Umkehr layers, so the pressure level picked was one within the corresponding Umkehr layer, but did not cover the entire layer, resulting in an approximation. We chose the pressure levels corresponding to Umkehr levels in the following way:

Table 2

Umkehr Layer	NMC Pressure Layer
2-3-4	150.0 mBar
5-6	10.0
7-8	5.0
9-10	1.0

Data Analysis

Examining the data for the various Umkehr layers, we see that the ozone plots of layer 2-3-4 and layer 5-6 show the amount of ozone over Antarctica decreases throughout the month of September staying low during October as expected. The ozone hole is pole-centered, extending out to about 65-70 latitude, and appears to rotate around the pole (fig. 2a and b) in conjunction with circulation changes [Schoeber et al,

1986].

Layer 7-8 has a region of less ozone centered above the South Pole, but, in agreement with Aikin and McPeters [1988], we find the amount of ozone actually increases during September contrary to what we find in the other layers. For example, on September 13 (fig. 5a), the ozone minimum is deeper than on October 1 (fig 1c) as the ozone levels increase from September 13 to October 1.

The ozone plots for layer 9-10 show the formation of an ozone minimum similar to layer 2-3-4, but which lags behind layer 2-3-4's ozone hole formation as well as an overall depletion during the months of September and October. Oct 1 (fig. 2d) is the beginning of the ozone decrease which reaches the minimum value by October 25 (fig. 6) in layer 9-10, while in layer 2-3-4 October 1 is the end of the time of ozone hole formation with the hole existing on into October. Another difference between layer 2-3-4 and layer 9-10 is that in layer 9-10 there is an overall decrease in ozone across the Southern Hemisphere coupled with the pole-centered region of ozone loss (compare again fig. 2d and fig. 6). It seems that there are two effects working here.

In layer 2-3-4, the area of ozone depletion is approximately the same size as the vortex and region of constant temperatures over Antarctica (see figures 2a, 3a, and 4a). Also, the rotation of the ozone hole is probably in conjunction with the vortex rotation. There is a correlation between the geopotential/ temperature plots and ozone plots in this layer as predicted since the geopotential/temperature plots show show the size of the vortex in which the PSCs are contained. Specifically, the winds are proportional in magnitude and perpendicular in direction to the gradient of the geopotential so the region of constant geopotential is the calm center while the region of high gradient is the edge of the vortex. Also, where the temperature is constant indicates a region of limited air mixing (fig. 3a) as it is contained within the polar vortex.

Even though the ozone plots of layer 5-6 are similar to layer 2-3-4 (compare fig. 2a and 2b), the temperature and geopotential plots are not. Instead, there is a smaller polar wind vortex (fig. 4b) and no region of temperature "vortex" (fig 3b). This may be explained by the fact that the temperature and geopotential structure mirrors that of layer 7-8 (see fig. 3b, 3c, 4b, 4c, 7 and 8) which has an even smaller polar vortex and a stronger geopotential gradient meaning higher winds as well as no central region of constant temperature. Therefore, the layer and pressure level match indicated in Table 2 for layer 5-6 may have resulted in inaccuracies causing this. On the other hand, since it is the transition region between the lower and upper layers, the plots may be accurate and layer 5-6 may have features of both.

In layer 7-8, the time when there is a strong temperature gradient (September 11-16) corresponds to the time of maximum ozone depletion (compare 5a and 5b with 2c and 3c). After this time, the minimum over Antarctica still exists, but ozone increases and the temperature contours show no vortex-type structure (see fig. 2c and 3c). In this layer, there is a strong correlation with the minimum ozone levels and the formation of a tight temperature gradient centered around the pole.

The geopotential data of layer 9-10 points to a small polar vortex not much larger than layer 7-8 and 5-6 meaning stronger winds than are in layer 2-3-4, but weaker than layer 7-8. However, the temperature is different and may explain the temperature structure of layer 7-8 and 5-6. The temperature structure is similar to layer 2-3-4 with a high temperature gradient surrounding a region of constant temperature. However, layer 9-10's gradient has a reverse sign of layer 9-10's. In other words, the temperature in layer 2-3-4 is cooler in the middle than on the edge of the vortex, but is reverse in layer 9-10. This explains layer 5-6 and 7-8's different temperature structure as they seem to be in the middle of this gradient inversion

from layer 2-3-4 to layer 9-10; hence, are transition layers.

Comparing more quantitatively the wind speeds at different levels and the shape of the polar vortex, we look briefly at the velocity of the winds of the polar vortex using the geopotential data. Fleming et al [1988] proposed the following equation relating the magnitude of the geopotential gradient with the wind as a rough estimate of the wind speed as a function of latitude:

$$\frac{[u]^2 \tan\theta}{a} + z\Omega[u]\sin\theta = -g_0 \frac{d[z]}{dy}$$

solving this yields,

$$[u] = -M + \sqrt{M^2 + 2M[u_g]}$$

[u] = zonal mean wind

$M = a\,\Omega\cos\theta$

$$[u_g] = \left(\frac{-g_0}{z\Omega\sin\theta}\right)\left(\frac{d[Z]}{dy}\right)$$

where a = Earth's radius

Ω = angular rotation of Earth

P = degrees latitude

[Z] = zonal average geopotential height

Comparing wind speed at the different levels using the equation listed above, we find higher wind speeds at higher altitudes (fig. 7). If the angular momentum of the vortex is conserved, then this is expected since at layers 7-8 and 9-10 there is much less mass and the radius is smaller.

Comparing the zonal mean temperature as a function of time for the different layers, we find that in the lowest and highest layers, the temperature stays constant (fig. 8). In layer 7-8 and layer 5-6, we see the springtime warming, not in layer 2-3-4 and layer 9-10. This may be a result of the depletion of ozone, especially in layer 2-3-4, since ozone warms the atmosphere as it absorbs ultraviolet rays as noted by Solomon [1988].

Conclusions:

From this quantitative analysis, we see that there is, as expected, a correlation between the ozone hole and the polar vortex as defined by the geopotential and temperature structure. In the lowest level, the ozone hole and vortex region are similar in size and position. The same is true of layer 9-10 which is similar to layer 2-3-4 except for the temperature gradient reversal and the overall ozone depletion that occurs in this layer. In both of these layers, the zonal mean temperature stays constant as a function of time, while in layer 7-8, it increases as springtime warming occurs. This, combined with the small polar vortex and lack of a constant temperature region, is probably part of the reason for the unusual behavior of the ozone: a stronger ozone minimum in September instead of October. Because PSCs are absent in layer 7-8 and 9-10,

we realize another mechanism is at work at these high altitudes as indicated by the different ozone minimum behavior at the different levels. The temperature information indicates that there is a correlation between the temperature structure and the ozone depletion so this mechanism causing the ozone minimum at higher levels will probably incorporate the relationship of the temperature and ozone structures.

Literature Cited

Aiken, A. C. and R. D. McPeters, The three-dimensional morphology of the Antarctic ozone minimum, *Geophysical Research Letters, 15*, 413-416, 1988.

Farman, J. C., B. G. Gardiner, and J. D. Shanklin, Large losses of total ozone in Antarctica reveal seasonal ClOx/NOx interaction, *Nature, 315*, 207-210, 1985.

Farmer, C. B., G. C. Toon, P. W. Schaper, J. F. Blavier, and L. L. Lowes, Stratospheric trace gases in spring 1986 Antarctic atmosphere, *Nature, 329*, 126-130, 1987.

Fleming, E. L., S. Chandra, M. R. Scoeberl, and J. J. Barnett, Monthly mean global climatology of temperature, wind, geopotential height and pressure for 0-120 km, *NASA Tech Memorandum 100697*, Feb. 1988.

Hamill, Patrick, O. B. Toon, R. P. Turco, Characteristics of PSCs during the formation of the Antarctic ozone hole, *Geophysical Research Letters, 13*, 1288-1291 1986.

Heath, D. F., C. L. Mateer, and A. J. Drueger, The Nimbus-4 Backscatter Ultraviolet (BUV) atmospheric ozone experiment - two years' operation, *PAGEOPH, 106-108*, 1238-1253, 1973.

Levi, B. G., Ozone depletion at the poles: the hole story emerges, *Physics Today, 41*(7), 17-21, 1988.

McCormick, M. P. , H. M. Steele, P. Hamill, W. P. Chu, and T. J. Swissler, Polar atmospheric cloud sightings by SAMII, *Journal of Atmospheric Sciences, 39*, 1387-1397, 1982.

McElroy, M. B. , R. J. Salawitch, S. C. Wofsy, and J. A. Logan, Reductions of Antarctic ozone due to synergistic interactions of chlorine and bromine, *Nature, 321*, 759-762, 1986.

McElroy, M. B. , R. J. Salawitch, and S. C. Wofsy,Chemistry of the Antarctic stratosphere, *Planetary and Space Science, 36*, 73-87, 1988.

Schoeberl, M. R. , A. J. Krueger, and P. A. Newman, The morphology of the Antarctic ozone hole as seen by TOMS, *Geophysical Research Letters, 13*, 1217-1220, 1986.

Solomon, S., The mystery of the Antarctic ozone "hole", *Review of Geophysics, 26*, 131-148, 1988.

Stolarski, R. S. , A. J. Krueger, M. R. Schoeberl, R. D. McPeters, P. A. J. C. Alpert, Nimbus-7 measurements of the springtime Antarctic ozone decrease, *Nature, 321*, 808-811 1986.

Turco, R. P. , O. B. Toon, and P. Hamill, Heterogeneous physicochemistry of the polar ozone hole, submitted to *Journal of Geophysical Research*, June 1988.

Fig. 2a: October 1, 1985 ozone plots for layer 2-3-4
(in Dobson units).

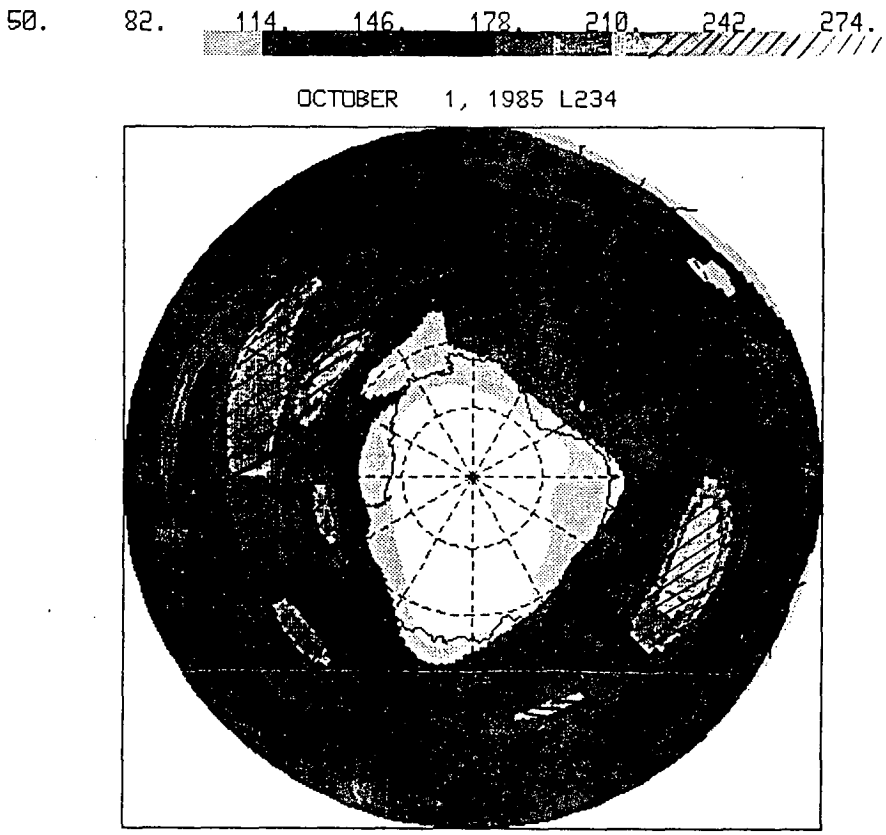

Fig. 2b: October 1, 1985 ozone plots for layer 5-6
(in Dobson units).

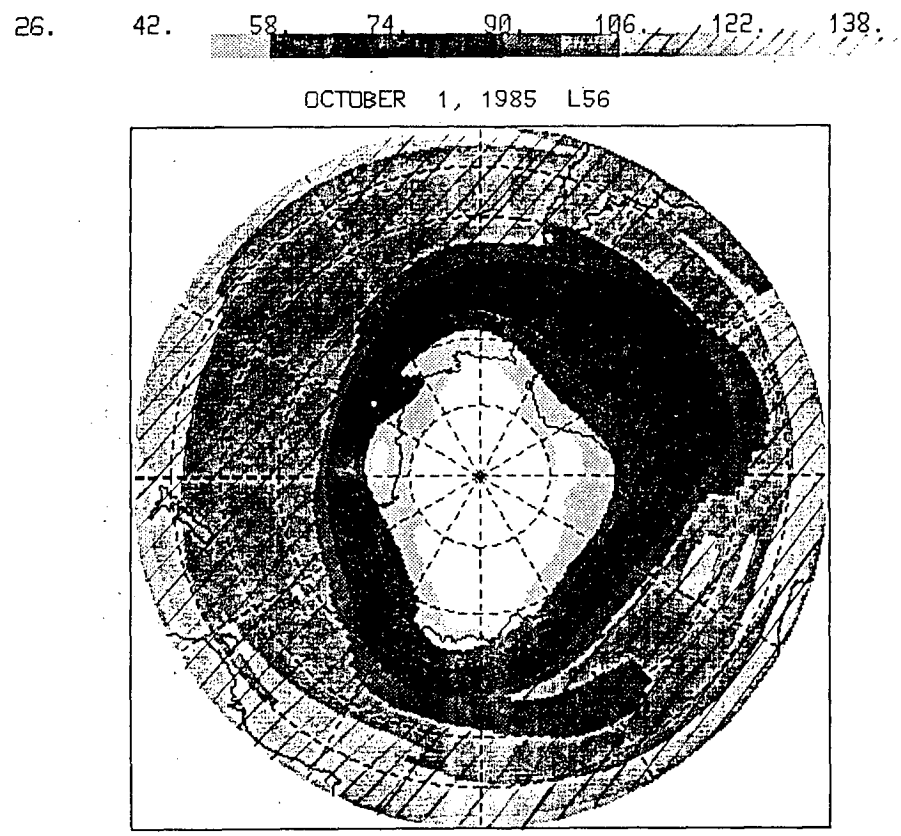

Fig. 2c: October 1, 1985 ozone plots for layer 7-8
(in Dobson units).

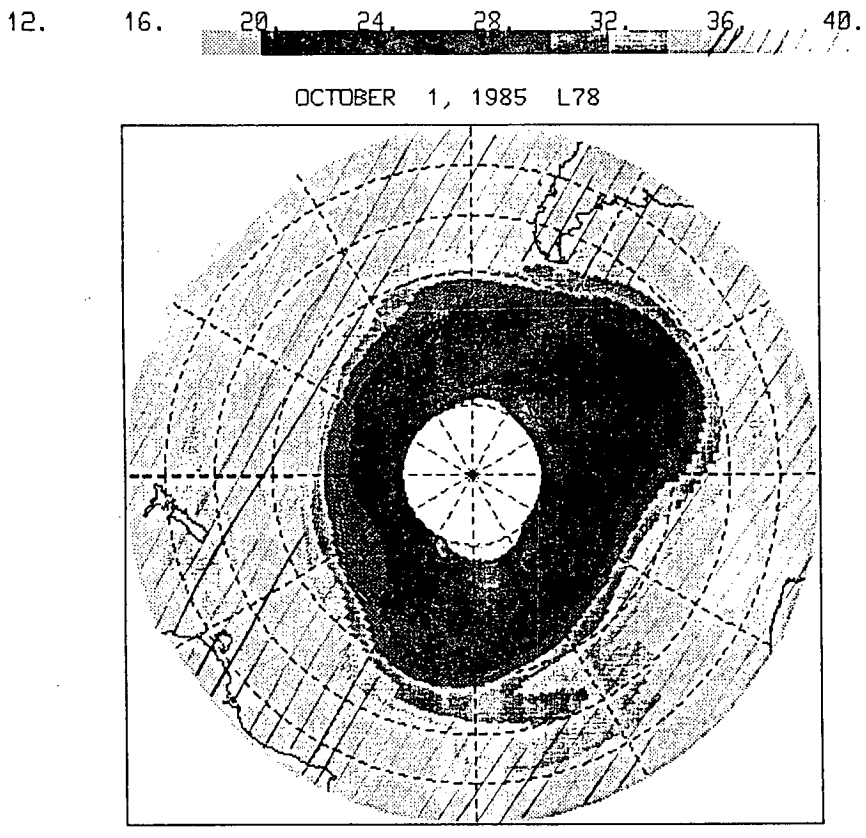

Fig. 2d: October 1, 1985 ozone plots for layer 9-10
(in Dobson units).

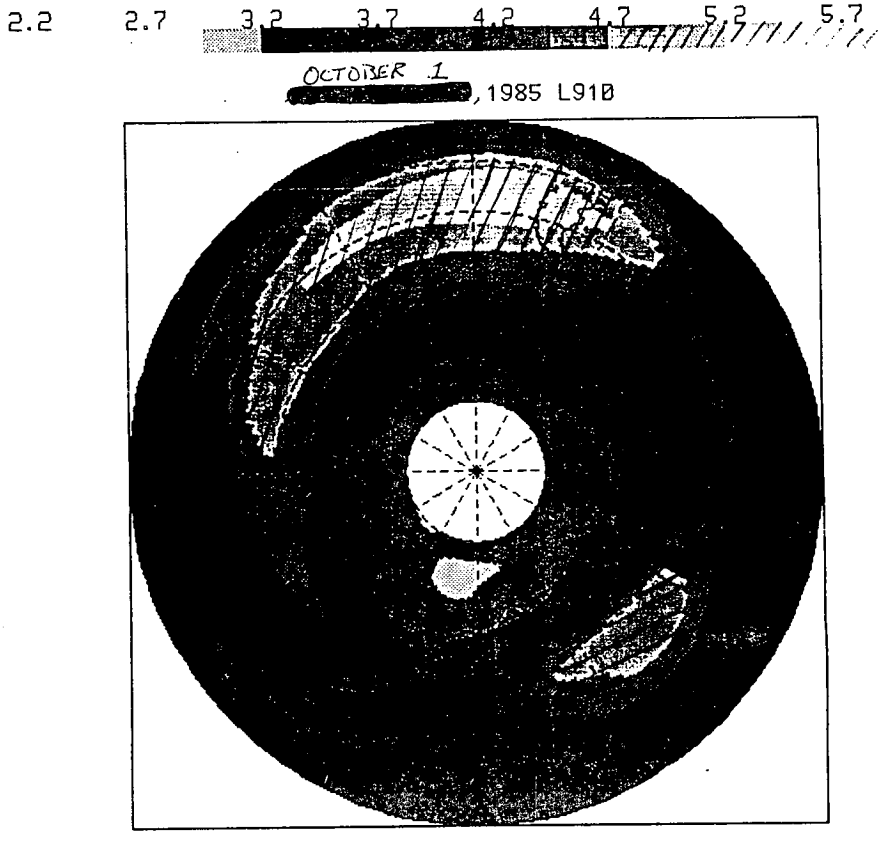

Figure 3a: October 1, 1985 NMC
Temperatures for 150.0 mBar

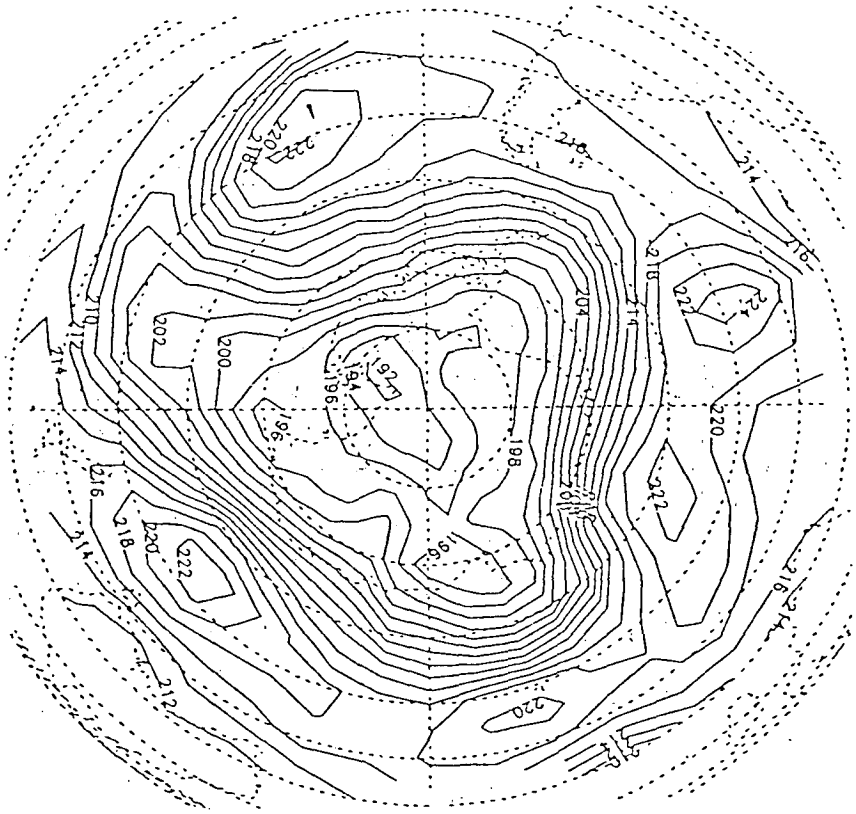

Figure 3b: October 1, 1985 NMC
Temperatures for 10.0 mBar

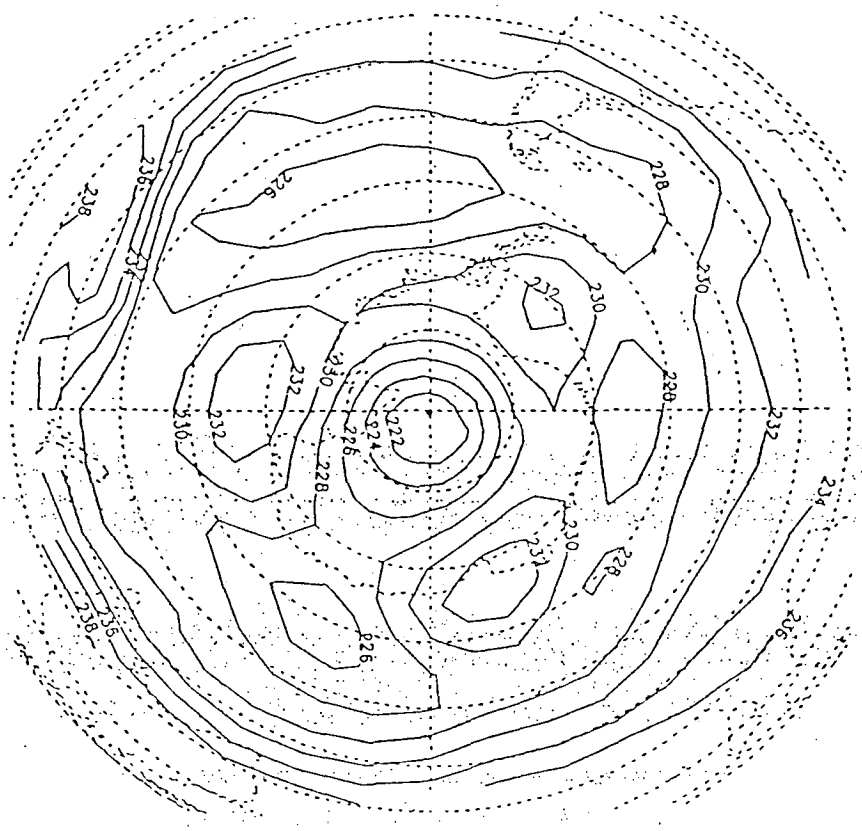

Figure 3c: October 1, 1985 NMC
Temperatures for 5.0 mBar

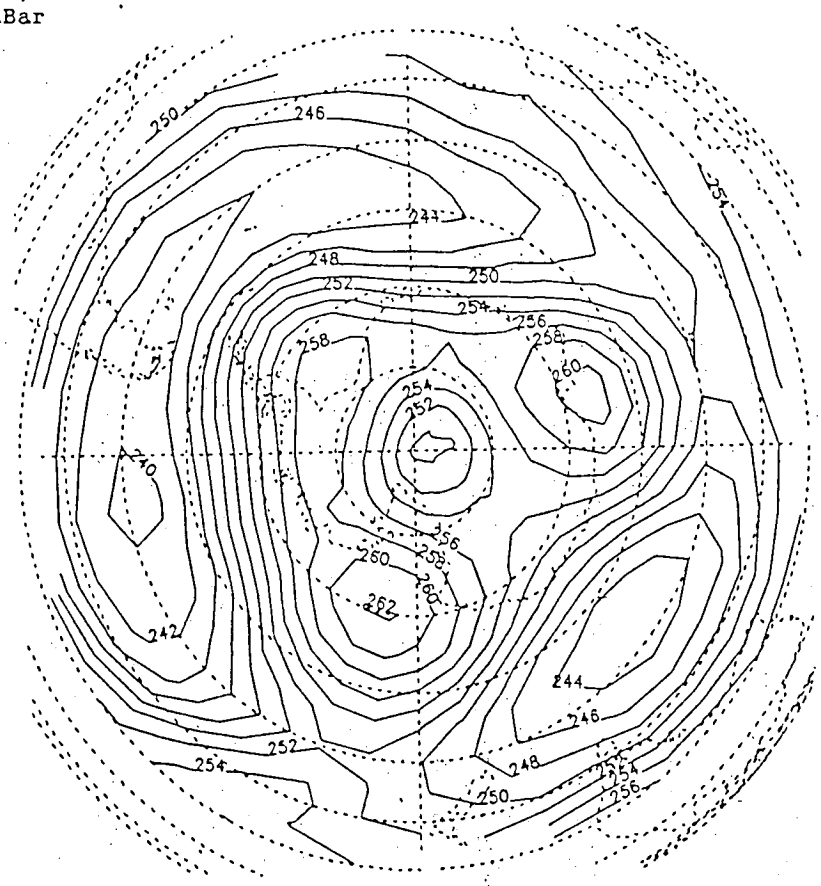

Figure 3d: October 1, 1985 NMC
Temperatures for 1.0 mBar

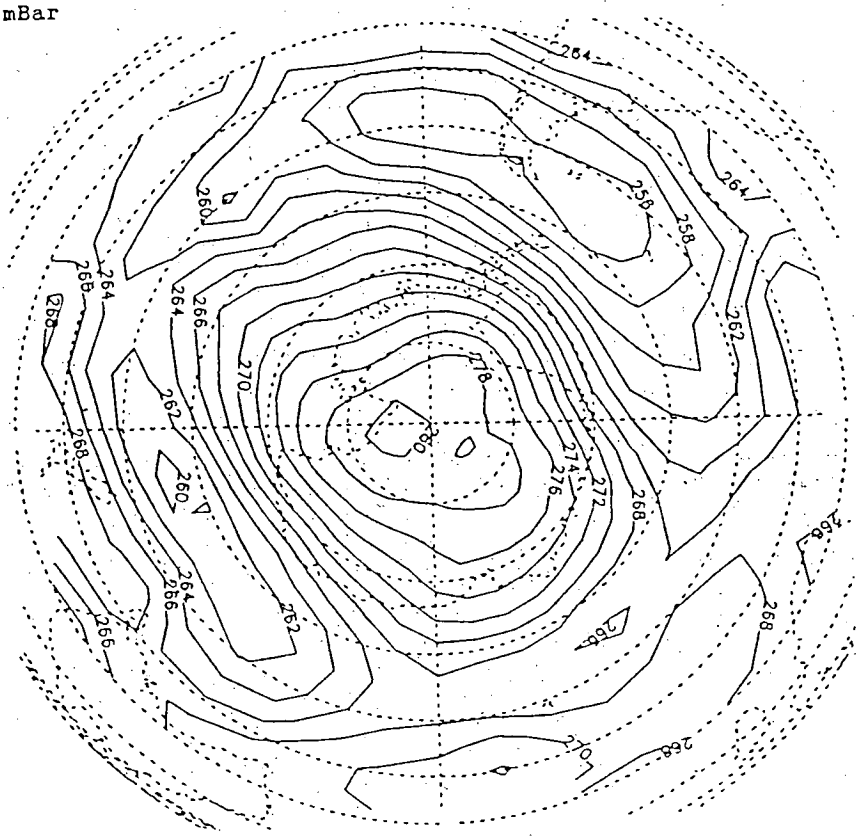

Figure 4a: October 1, 1985 NMC
Geopotentials for 150.0 mBar

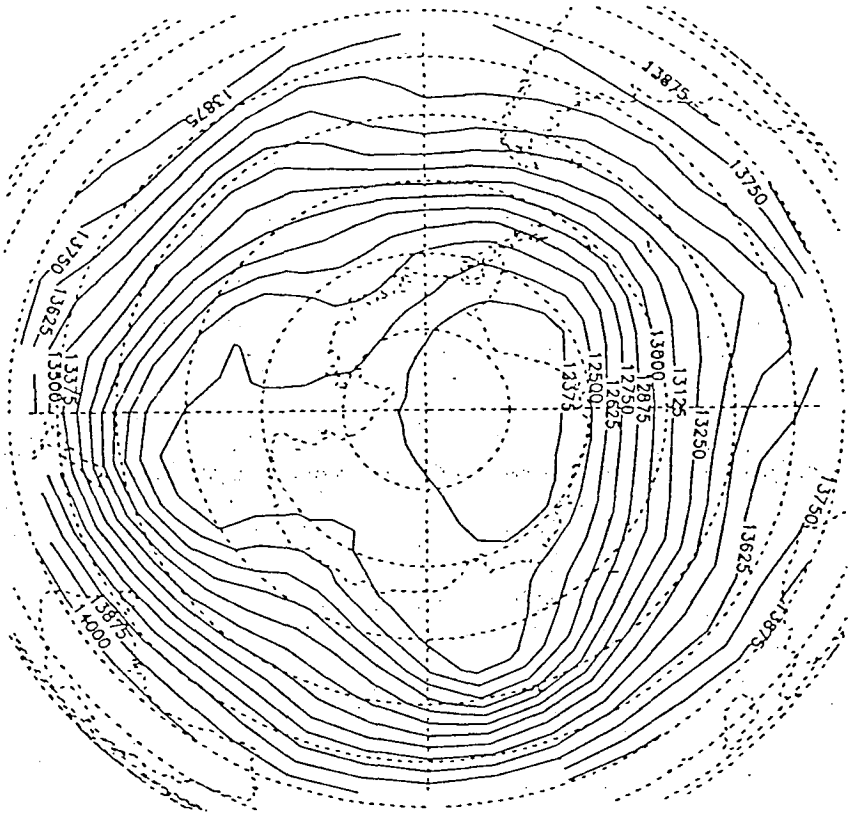

Figure 4b: October 1, 1985 NMC
Geopotentials for 10.0 mBar

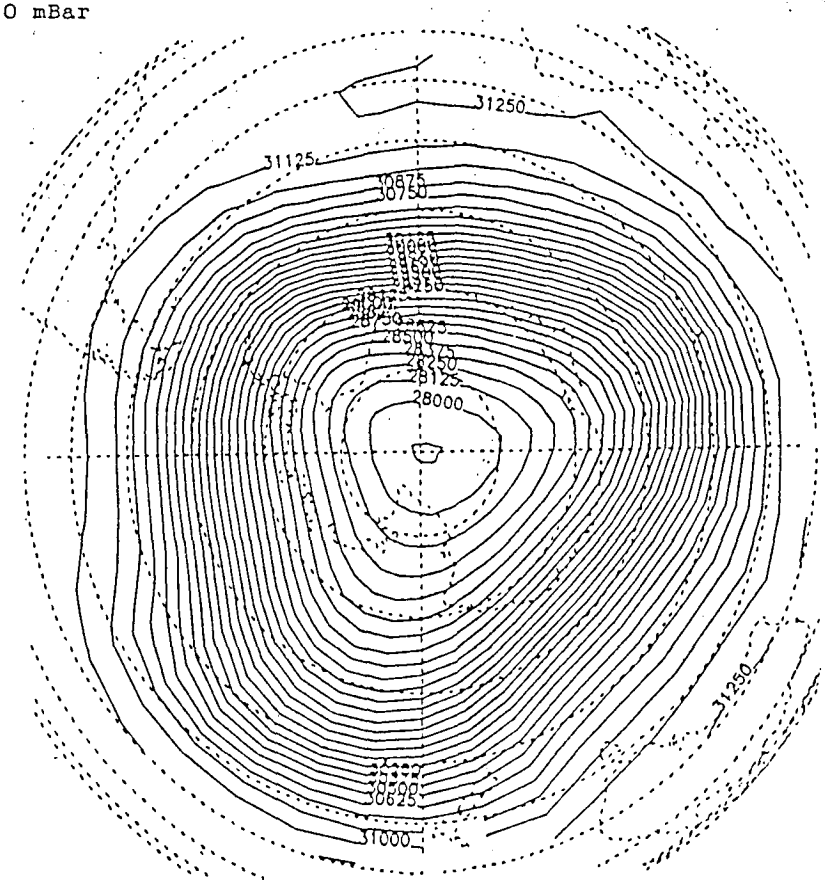

Figure 4c: October 1, 1985 NMC
Geopotentials for 5.0 mBar

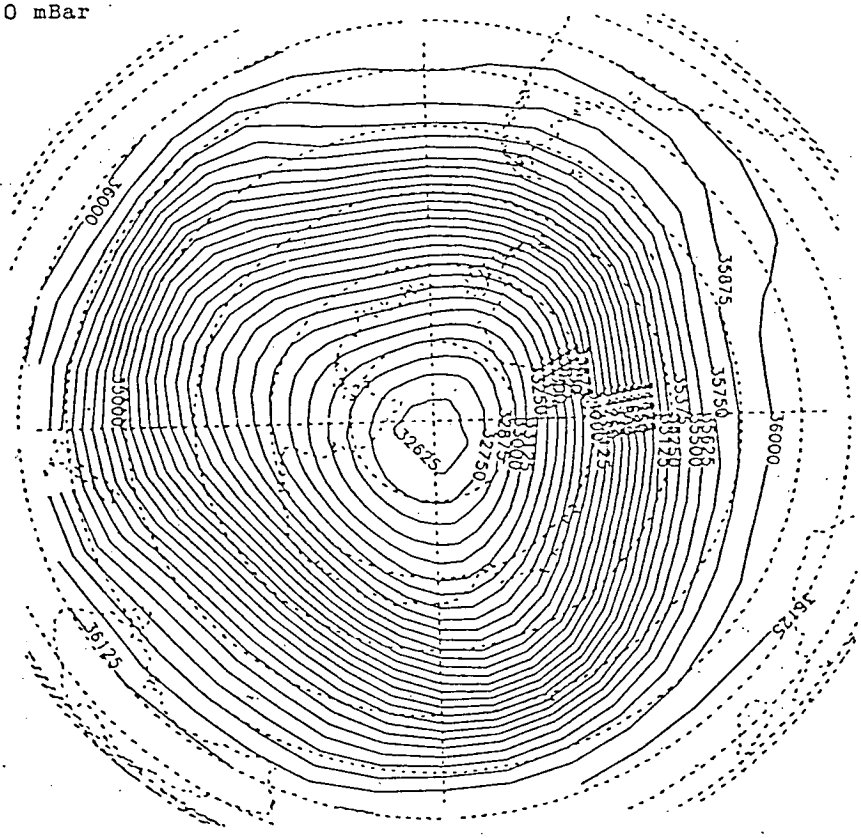

Figure 4d: October 1, 1985 NMC
Geopotentials for 1.0 mBar

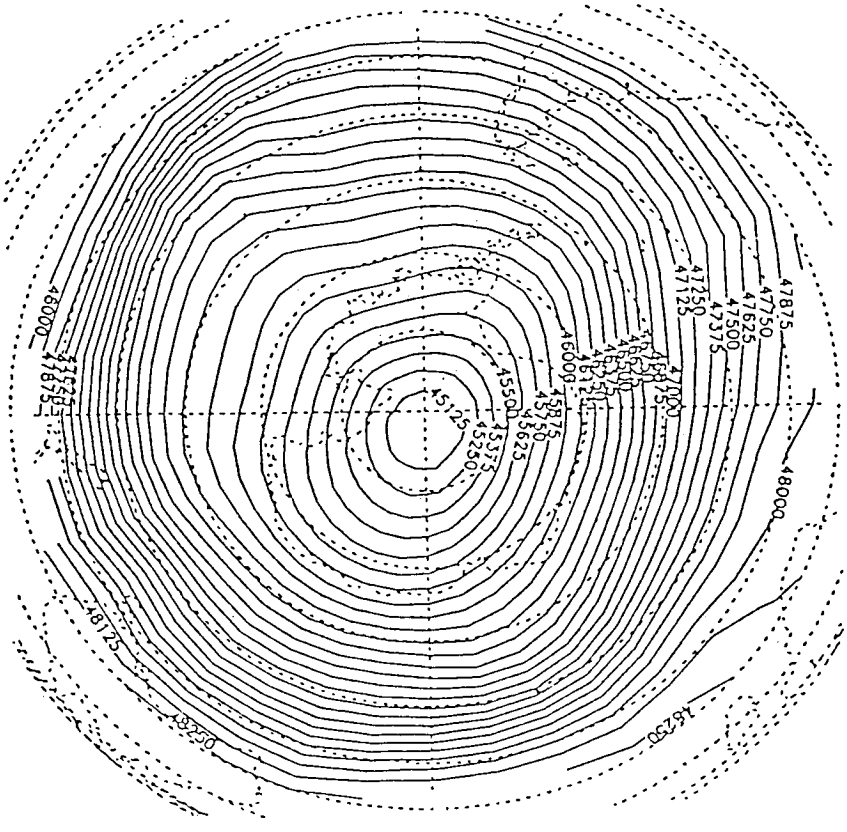

Fig. 5a: September 13, 1985 ozone plots for layer 7-8
(in Dobson units).

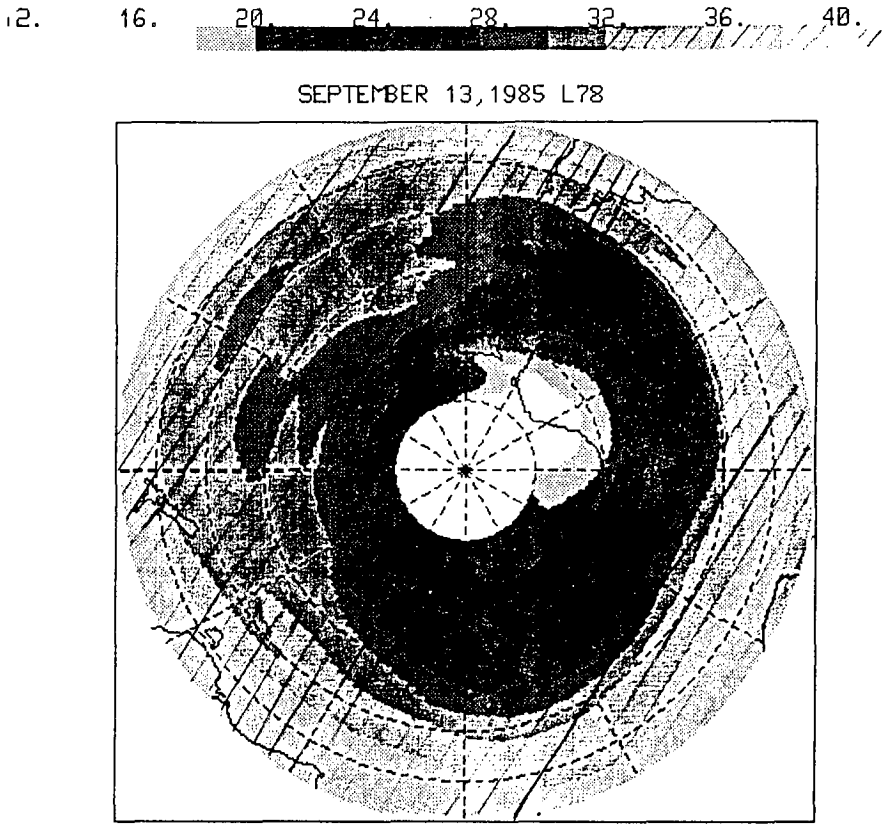

Figure 5b: September 13, 1985 NMC
Temperatures for 5.0 mBar

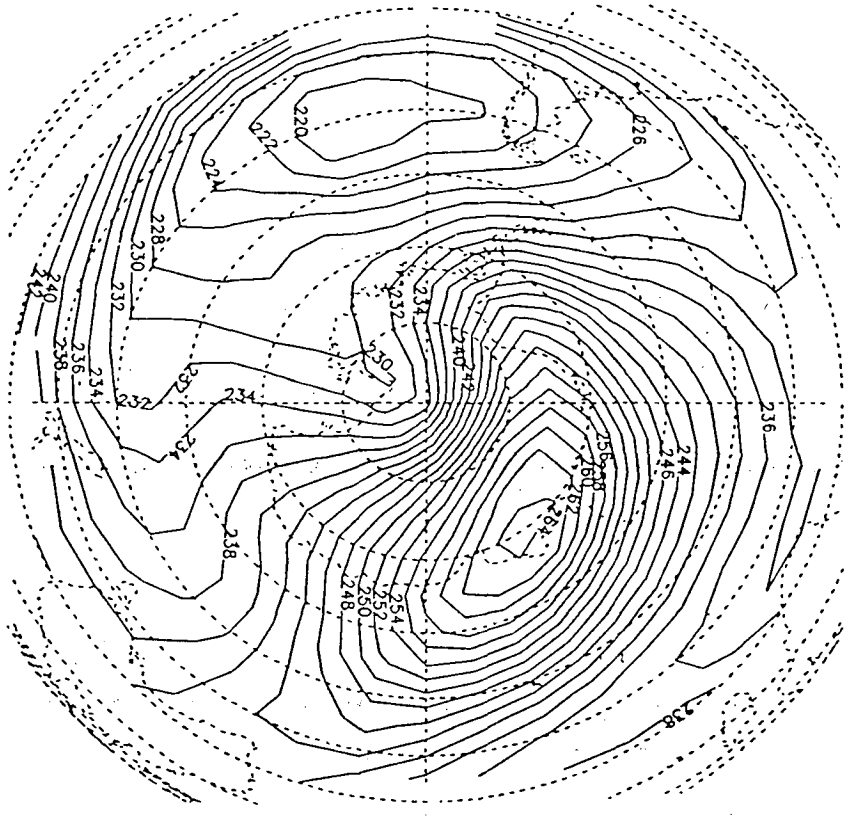

Fig. 6: October 28, 1985 ozone plots for layer 9-10 (in Dobson units).

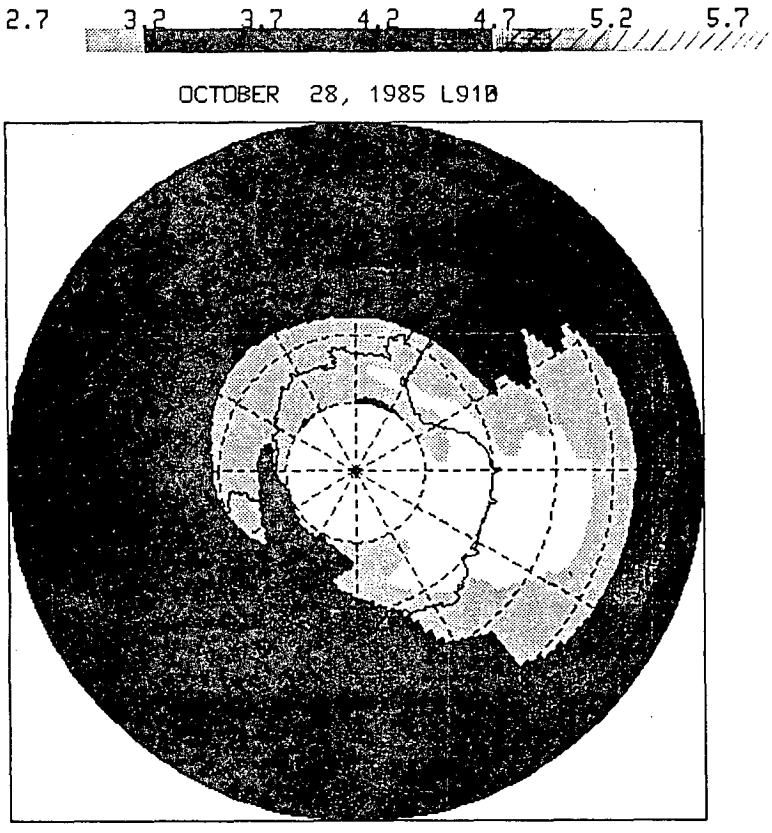

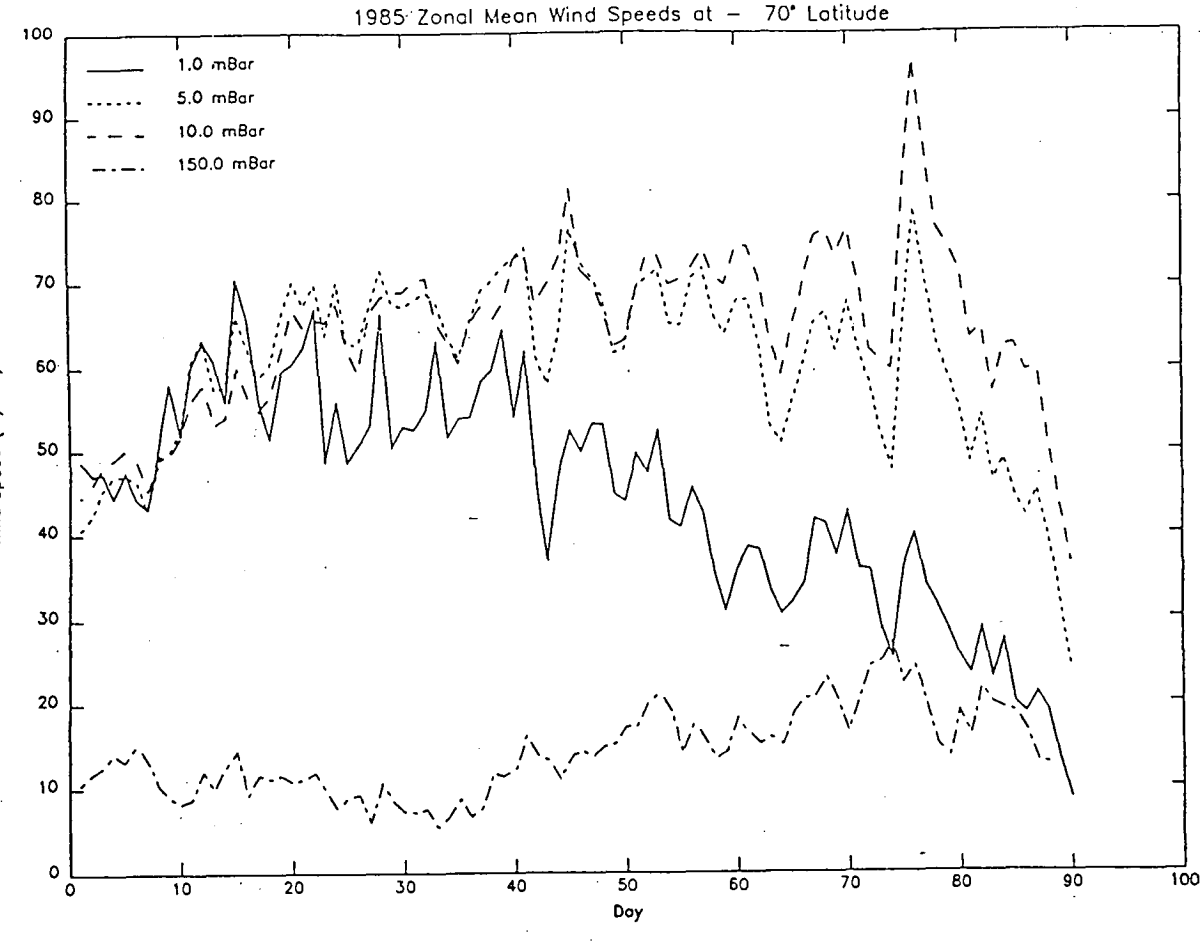

Figure 7: Zonal mean winds speeds at 70 degrees South vs. time for August-October, 1985.

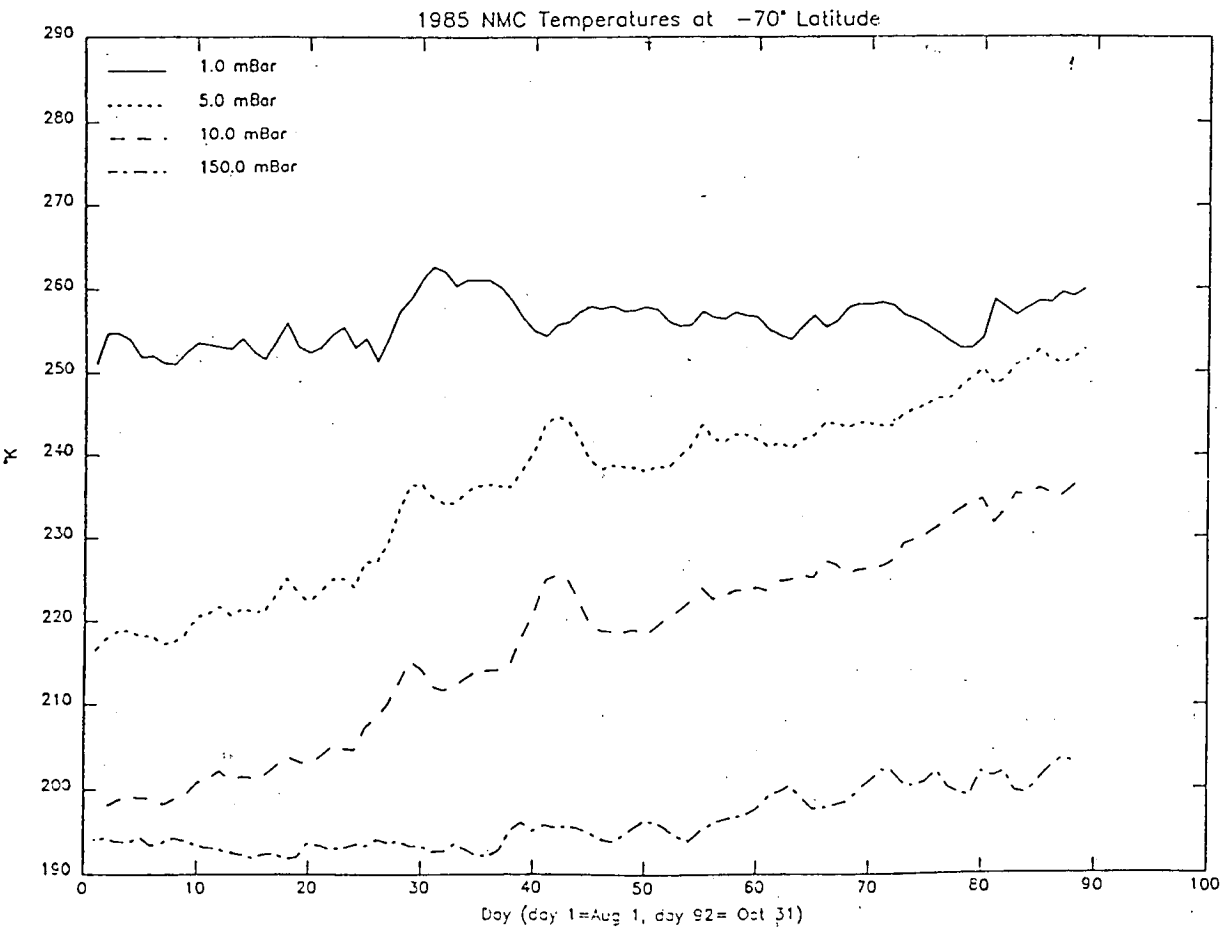

Figure 8: Zonal mean temperatures at 70 degrees South vs. time for August-October, 1985.

QUANTITATIVE ANALYSIS OF IMPURITIES IN VARIOUS ALCOHOLS USING AN INTERNAL STANDARD TECHNIQUE

Bruce K. Kellerman†

Abstract

The use of an internal standard and gas chromatography revealed quantitative information about the number and amounts of certain organic impurities present in gin, rum, scotch, vodka, and whisky. Ethyl acetate, 2-methyl-1-propanol, 3-methyl-1-butanol, and n-propanol were the impurities found in the various alcohols (Rice, 1987). Scotch and whisky contained all four impurities, while rum contained only three. The two colorless alcohols, gin and vodka, were relatively pure.

Introduction

The amount of amyl alcohol impurities, fusel oil, in alcoholic beverages is thought to be directly related to the hangover suffered after drinking an excess of the alcohol. Rice demonstrated that ethyl acetate, 2-methyl-1-propanol, 3-methyl-1-butanol, 2-methyl-1-butanol, and n-propanol are common impurities found in distilled alcohols (Rice, 1987). Rice developed a procedure using a gas chromatograph to separate these impurities in a whisky sample (Rice, 1987). Our procedure differs from Rice's, however, and is exzpanded to include an analysis of gin, rum, scotch, and vodka as well as whisky.

In this lab, gas chromatography was utilized in order to determine the number of impurities present in each alcohol, while the internal standard, 1-butanol, was used to determine the amount of each impurity present. 1-butanol was chosen as the internal standard because it is similar to the analytes (i. e., impurities) and does not interfere with the analytes. Also, since the response of the analytes and 1-butanol are affected similarly, 1-butanol was chosen as the internal standard.

Procedures

A Hewlett Packard model 5890 A gas chromatograph equipped with an HP-20M carbowax capillary column was used. A flame ionization detector was used, and nitrogen served as the carrier gas. The injection and detection temperatures were maintained at 200 ^{o}C, while the oven temperature was programmed from 60^{o}C to 160^{o}C at a rate of 8^{o}C/min.

A standard solution consisting of 40% ethanol in water, 1-butanol (the internal standard), and ethyl acetate, 2-methyl-1-butanol, 3-methyl-1-butanol, n-propanol, 2-methyl-1-propanol (the impurities) was made. Each solution contained 25 microliters of each analyte and 25 microliters of the internal standard in a 50 ml solution. A volume of 25 microliters in a 50 ml solution corresponds to a concentration of 500 parts per million (ppm) of that component. Therefore, 50 ml solutions of each alcohol containing 25 microliters of 1-butanol were prepared. Thus, each solution used consisted of 500 ppm of 1-butanol.

† Bruce is a senior Chemistry major from Saint Louis, MO.

Volumes of less than 0.1 microliter of each solution (the standard solution and alcohol solutions) were injected into the gas chromatograph. Nine gas chromatograms of the standard solution were obtained in order to determine a relatively accurate response factor for each impurity (See Results and Discussion). Figure I contains a sample gas chromatogram of the standard solution. Each peak is labeled according to its retention time. The gas chromatograms obtained for each alcohol (not shown) contained the internal standard in the amount of 500 ppm. Therefore, the amounts of each impurity were calculated using their response factors and areas under each peak (See Results and Discussion).

Figure 1
Sample gas chromatogram of the standard solution.

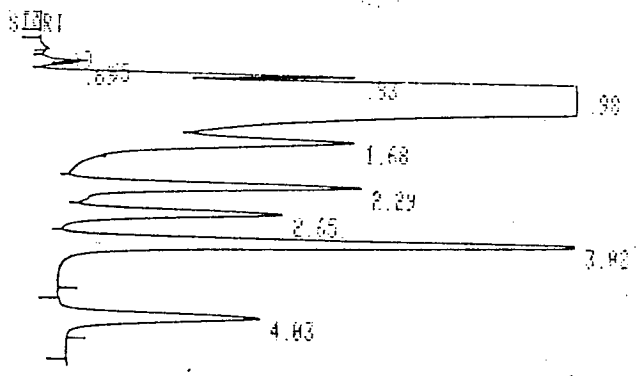

Peak Identification: 0.83, ethyl acetate; 0.98, ethanol; 1.68, n-propanol; 2.29, 2-methyl-1-propanol; 2.65, 2-methyl-1-butanol; 3.02, 1-butanol; 4.03, 3-methyl-1-butanol. This chromatogram contains 500 ppm of each impurity.

Discussion

It is clear from Figure I that even though the standard solution contains equivalent amounts of each analyte, the response is not the same. Therefore, response factors must be determined for each analyte relative to the internal standard. The response ratio of analyte to internal standard is determined by the following equation (Rice, 1987):

$$F = \frac{(A/W)_c}{(A/W)_{is}} \qquad (1)$$

where $(A/W)_c$ = area and weight for analyte,

$(A/W)_{is}$ = area and weight for internal standard, and

F = response factor.

Since 500 ppm is taken as the weight of each component, equation (1) simply reduces to the ratio of the area of the analyte over the area of the internal standard. Thus response factors can be easily determined and the resulting response factors for each analyte can be found in Table I. The average deviations for 2-methyl-1-butanol, 3-methyl-1-butanol, and 2-methyl-1-propanol were all within 2% of the average response factor. However, the average deviations for n-propanol and

ethyl acetate were within 10.1% and 7.1%, respectively, of their average response factor.

Once response factors for each analyte had been calculated, they were used to determine the amounts of each impurity in the various alcohols through a simple rearrangement of equation (1):

$$Wc = \frac{Wis * Ac}{Fc * Ais} \qquad (2)$$

Since the amount of internal standard added to each alcohol sample was 25 microliters/50 ml of solution, W_{is} = 500 ppm for every sample. The area of the impurity and the area of the internal standard were obtained from the gas chromatograms, and F_c was previously determined using the standard solution. Table II contains the results obtained from this experiment. Vodka was found to be "pure," while gin contained one impurity, ethyl acetate, in a very small amount. Scotch and whisky contained four organic impurities each, the whisky possesses these impurities in larger amounts. Note the amount of 3-methyl-1-butanol present in the whisky.

The experimental data was obtained using only one brand of each alcohol. These results should not be generalized to include all brands of the same alcohol.

Table I
Response Factors of Each Analyte

Analyte	Retention Time	Avg. Response Time	Avg. Deviation
ethyl acetate	0.83	0.490	0.035
n-propanol	1.68	0.634	0.064
2-methyl-1-propanol	2.29	0.999	0.017
3-methyl-1-butanol	4.03	0.725	0.014
2-methyl-1-butanol	2.65	0.740	0.012

Table II
ppm Levels of Impurities in the Alcohols

Impurity	GIN	RUM	SCOTCH	VODKA	WHISKEY
ethyl acetate	14	124	229	—	514
n-propanol	–	—	358	—	149
2-methyl-1-propanol	–	31	360	—	1261
3-methyl-1-butanol	–	210	299	—	4941

Literature Cited

Gary W. Rice, Determination of Impurities in Whisky Using Internal Standard Techniques. *Journal of Chemical Education, 64 , Number 12,* Dec. 1987.

An Experimental Study of the Effects of Rifampicin on *E. coli* Protein Synthesis Using Liquid Scintillation Spectroscopy

R. B. Reed†
W. Raymond Brown††
William T. Holden†††
Salil P. Parikh††††

Abstract

The use of liquid scintillation spectroscopy provided much insight into the effects of the antibacterial agent, rifampicin, upon protein systhesis in E. Coli cells. Following the incorporation of tritiated leucine into the cells, liquid scintillation spectroscopy was used to quantify the extent of protein synthesis occurring in rifampicin-treated cells as compared with control cells. from these studies, it was concluded that rifampicin is an inhibitor of protein synthesis in the bacterial cells studied.

Introduction

A radiotracer is an organic molecule composed of radioactive atoms that can be used to identify specific members of a molecular population. Radioactive tritium (^3H) is often used in probing biological systems due to its relatively long half-life (12.26 yrs.), its ease of introduction into organic molecules, and the ability to detect and measure the low energy ß-radiation it emits during decay.

Tritiated leucine, ^3H-leu, a radioactive amino acid, will be taken up from the culture medium into the *E. coli* bacterium as it synthesizes proteins containing leucine in their amino acid sequences. A culture containing rifampicin can also be made, and under identical conditions to the control culture, the effects of rifampicin on the uptake of ^3H-leu into *E. coli* will be examined. Used clinically as a therapeutic agent against tuberculosis and various tumors, rifampicin has also been shown to have anti-bacterial potency (Lester, 1972). Ultimately, use of the specific activity of the labelled amino acid will help to determine the amount of incorporation of ^3H-leu into *E. coli* proteins, both in the presence and absence of rifampicin, and some generalizations about protein synthesis in *E. coli* proteins using ^3H-leucan then be drawn.

This incorporation of radioactive leucine can be measured and quantified using liquid scintillation spectroscopy (LS) which has a relatively high efficiency for detecting the ß-radiation that tritium emits during decay. LS quantifies the amount of radioactivity present in a sample by counting the number of emissions detected (expressed as counts per minute, or CPM). Due to the inherent inefficiencies of the liquid scintillator and the weakness of the tritium ß-rays, only about 40-50% of the actual number of emissions (disintegrations per minute, or DPM) is able to be detected and counted (CPM).

---

† Bobby is a senior chemistry major from Clarksville, Tennessee.
††Ray is a senior chemistry major from Knoxville, Tennessee.
†††William is a senior biology major from Memphis, Tennessee.
†††† Salil is a senior chemistry major from Memphis, Tennessee.

The largest source of system inefficiency arises from a phenomenon known as percent quenching. Essentially, in biological samples, additional matter diminishes the intensity of ß-rays emitted, thereby lowering the efficiency of the detector. Quenching also alters or shifts the spectra of energies. These problems may be somewhat overcome by creating a "quenching curve" or standard curve used to determine the efficiency of each individual sample.

Standards whose quenching effects are known are read for CPM and compared to an external standard ratio (ESR) to create the curve. The ESR is directly proportional to the efficiency so that the ESR of each sample can be used to determine the efficiency for that sample. Indirectly, the DPM of all samples can be calculated, and used in an analysis of the incorporation of ^{3}H-leu into *E. coli* proteins, and the effect, if any, of rifampicin upon that incorporation.

Materials and Methods

The radioactive leucine was first incorporated into the E. coli using a slightly modified experimental prcedure (Cooper, 1971). A culture of wild type *E. coli* of an approximate cell density of 45 klett units was incubated with 2mM ^{3}H-leucine in a 30 C water bath. At specified time intervals, 0.2ml samples of the experimental solution were removed in triplicate and added to 5% trichloroacetic acid (TCA) to precipitate nucleic acids and proteins. Simultaneously, samples were extracted from a second reaction mixture containing 0.1ml of a 10µmol/ml solution of rifampicin.

After all samples (experimental and control) had been collected at the specified time intervals, they were placed in a boiling water bath to release the ^{3}H-leu from the tRNA. After the samples were cooled on ice, the protein and nucleic acid precipitations were collected by filtration. The filter papers containing the radioactive proteins and the non-radioactive nucleic acids were dried at 70 C overnight to remove the TCA which could interfere with liquid scintillation. The filters were then placed into scintillation vials along with 15ml of scintillation fluid. After 24 hours of incubation, each solution was read for radioactivity using a liquid scintillation spectrophotometer. Simultaneously, a set of quenching standards was also read and a quench curve constructed.

Results

Since the radioactive standards decay over time, the following formula was used

$$\log \frac{A_0}{A_t} = \frac{0.3t}{T_{1/2}}$$

to determine how many disintegrations per minute we expected to be present on the day the standards were counted using the LS. If A_o on February, 9, 1968 (the day the standards were irradiated) equals 455,000 DPM, then as of October 12, 1988 (the day the standards and samples were read), t= 20.67 years and A_t therefore was

$$\text{Log } \frac{455{,}000}{A_t} = \frac{0.3\ (20.67\text{yrs})}{12.26\ \text{yrs}}\ ; \quad A_t = 141{,}978\ \text{DPM}.$$

The actual number of counts detected by the LS spectrometer (CPM) divided by the actual number of emissions (A_t) is the efficiency of each standard. The ESR, which is a ratio of counts in two energy windows and is proportional to the amount of quenching, was provided by the spectrometer. The data below were used to construct the quenching curve that will enable us to determine the efficiency of each of our collected samples.

Table 1

Quenching Curve Data from Standards

Sample #	CPM	Efficiency (CPM/A_t)	ESR
151	90357	0.64	3.827
152	82641	0.58	3.372
153	67971	0.48	2.681
154	51118	0.36	2.151
155	35997	0.25	1.700
156	15630	0.11	1.066
157	12596	0.09	0.967

The equation for the best straight line through the standard points was **y = 0.1979006x - 0.0871007**, with a correlation coefficient of **0.99461**, using the standards numbered 151-157.

Figure 1
Quench Curve
(Standard Curve)

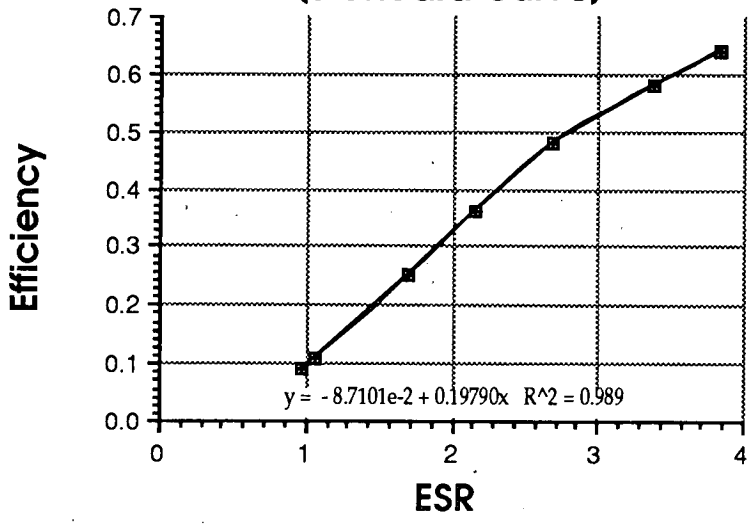

Our group data derived from samples numbered 158-181 are listed below, separated into rifampicin-treated and rifampicin-free categories.

Table 2

Rifampicin Free:

Time	Sample #	CPM	ESR	Efficiency	DPM (CPM/Eff)
5	158	22	2.936	0.49	45
	159	279	2.851	0.48	581
	160	266	2.852	0.48	554
10	161	347	2.838	0.47	845
	162	152	2.994	0.51	298
	163	388	2.844	0.48	808
20	167	1004	2.842	0.48	2092
	168	824	2.885	0.48	1717
	169	885	2.868	0.48	1844
30	173	1345	2.910	0.49	2745
	174	1382	2.920	0.49	2820
	175	1248	2.805	0.47	2655
40	179	1900	2.800	0.47	4043
	180	1702	2.893	0.49	3473
	181	1820	2.775	0.46	3957

Table 3

Rifampicin Treated:

Time	Sample #	CPM	ESR	Efficiency	DPM (CPM/Eff)
15	164	586	2.944	0.50	1172
	165	647	2.898	0.49	1320
	166	569	2.848	0.48	1185
25	170	643	2.879	0.48	1340
	171	732	2.950	0.50	1464
	172	707	3.004	0.51	1386
35	176	791	2.943	0.50	1582
	177	749	2.968	0.50	1498
	178	797	2.910	0.49	1627

From the average of the DPM's of each given time, we calculated the activities of all the samples, and reported them in terms of microcuries (μCi). By definition, 1 μCi of radioactivity is that which produces 2.22×10^6 DPM. To find

the molar quantity of ^{3}H-leucine assimilated into each sample, we simply used the fact that the tritium-labelled leucine has a specific activity of 1 μCi/μmol. For example, for the average value of DPM of the sample taken at 20 min, we found 8.49 x10^{-4}μmol of ^{3}H-leu incorporated into the *E. coli*.

Example Calculation: $\frac{(1884\ \text{DPM})\quad(1\mu\text{Ci})\quad(1\mu\text{mol})}{(2.22 \times 10^6\ \text{DPM})\quad(1\mu\text{Ci})} = 8.49 \times 10^{-4}\ \mu\text{mol}$

The table below lists the average DPM's of the three samples taken at each time followed by their respective molar quantities of ^{3}H-leu assimilated into *E. coli* .

Table 4

Rifampicin-Free

Time (min)	Average DPM	Quantity of leu incorporated (X10^{-4} μmol)
5*	568	2.56
10*	827	3.73
20	1884	8.49
30	2740	12.3
40	3824	17.2

Rifampicin-Treated

Time (min)	Average DPM	Quantity of leu incorporated (X10^{-4} μmol)
15	1226	5.52
25	1397	6.29
35	1569	7.07

* One value of DPM was omitted for average calculations due to its apparently obvious deviation from the other two values. These values are shown in Table 2.

Figure 2

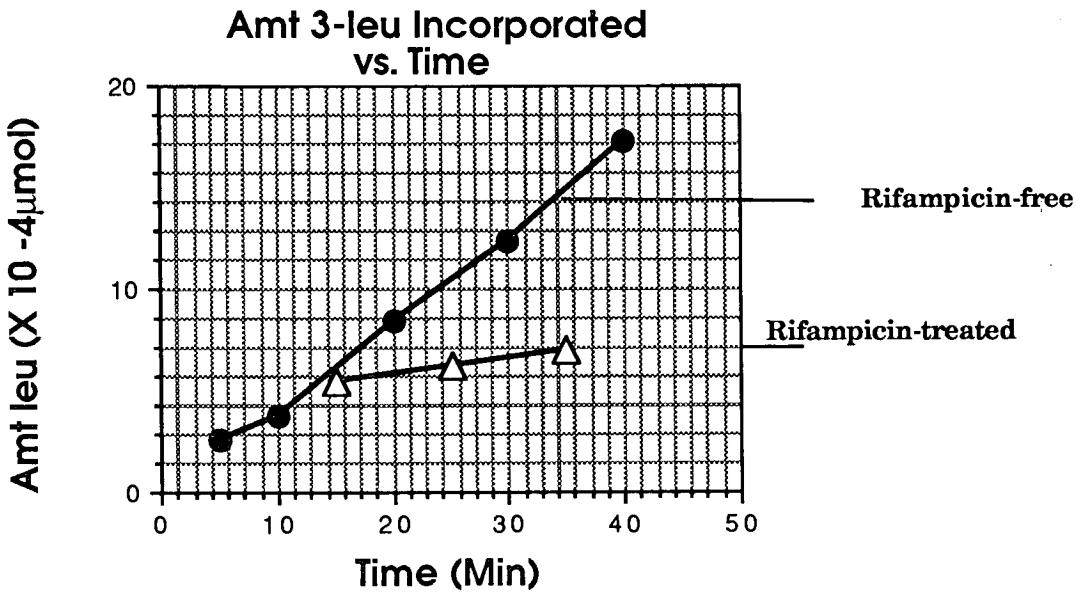

An average rate of assimilation may be found for both the treated and untreated samples by simply subtracting the molar quantity of the last sample taken from that of the first sample taken and dividing by the time elapsed between the two samples. Therefore, for the rifampicin-free sample, its average incorporation rate was

$$\frac{(17.26 \times 10) - (4 - 2.56 \times 10^{-4})\ \mu mol}{35\ min} = 4.18 \times 10^{-5}\ \mu mol/min$$

Likewise for the treated sample, the average incorporation rate was

$$\frac{(7.07 \times 10^{-4}) - (5.52 \times 10^{-4})\ \mu mol}{20\ min} = 7.75 \times 10^{-6}\ \mu mol/min.$$

This corresponds to roughly an 80% reduction of incorporation caused by the addition of rifampicin.

Discussion

The graph of the amount of ^{3}H-leu incorporated versus time for rifampicin-treated and rifampicin-free samples (Fig. 2) provides useful information for an analysis of the effects of rifampicin on the introduction of ^{3}H-leucine into *E. coli.* Each line appears to be nearly linear, but the slopes differ notably. The slope of the rifampicin-free line increases significantly with time so that as time is doubled so, too, does the height of the line, thus indicating a constant intake of labelled leucine into the cell and consequently a constant rate of protein synthesis. Over time, the rifampicin-treated line fails to increase its height at any rate comparable to the rifampicin-free line, thus implying that rifampicin somehow slows the rate of assimilation of labelled leucine and consequently protein synthesis.

The most likely explanation is that rifampicin somehow inhibits protein synthesis in *E. coli* . This would explain the lack of incorporation shown in figure 2, since the cell could no longer use leucine. According to Peberdy (1980), RNA polymerases are subject to inhibition by rifampicin, which binds specifically to a subunit of the enzyme core. It was Wu (1976) who proposed that rifampicin binds to the ß -subunit in *Escherichia coli* . Rifampicin binding to the ß-subunit of bacterial RNA polymerase results in the inhibition of transcription initation (Buss et al., 1978). This leads to inhibition of protein synthesis and then, ultimately, to the death of the cells if allowed to persist (Riva and Silvestri, 1972).

The literature supports our theory that rifampicin directly impedes protein synthesis as shown by the lack of assimilation of labelled leucine in rifampicin-treated cells as compared with non-treated cells. In this experiment, rifampicin served to decrease the average rate of incorporation to approximately 20% of the normal rate as calculated from data obtained using liquid scintillation spectroscopy.

There are numerous posibilities of student error in this experiment. Failure to pipet the exact amounts of reagents, neglecting to mix reagents thoroughly, and deliquency in withdrawing samples at the correct time intervals are among the most probable sources of random error in this experiment. Also, systematic error could possibly exist in the liquid scintillation spectrometer. However, these error sources can be seen as negligible. The data, therefore, can be accepted with some degree of confidence.

Acknowledgements

Special recognition should be granted to Anne-Marie Bassarrate, Lora Lofties, Josh McCanless, Todd Meyer, Barbara Mulach, Rakesh Patel, and Harold Wright whose subsequent experimental data served to aid in the conclusions of this experiment. In addition, Dr. Terry Hill should be thanked for his help in interpreting the data.

Literature Cited

Buss, W. C., et al. 1978. **Rifampicin Inhibition of Protein Synthesis in Mammalian Cells.** *Science, 200* pp. 432-4.

Lester, William. 1972. **Rifampicin: A Semi-synthetic Derivative of Rifamycin-A Prototype for the Future.** *Annual Review of Microbiology. 26.* Palo Alto,California:Annual Reviews, Inc. p. 90

Peberdy, J.F. 1980. *Developmental Microbiology.* New York: John Wiley & sons, p. 103.

Riva, S. and L. G. Silvestri. 1972. **Rifamycins : A General View.** *Annual Review of Microbiology. 26* . Palo Alto, California: Annual Reviews, Inc. p. 199.

Wu, Cheng-Weu. 1976. **Spatial Relationship of the Sigma Subunit and the Rifampicin Binding site in RNA Polymerase of *E.Coli*.** *Biochemistry* 15 (10), pp. 2097-2104.

Mother-Infant Interaction During Feeding Episodes: A Comparison of Breast- and Bottle-Feeding Dyads

Lori Vallelunga†

Abstract

Videotapes were made of twelve mothers with their 5- to 14-week-old first borns. Half of the mothers were total breastfeeders and half had never breastfed. Eight maternal and seven infant behaviors were coded and the frequency, duration, and sequencing of those behaviors were compared for the two groups. Matrices of transitional probabilities were constructed for each group and models were developed representing the relative frequency of the observed behaviors and the probability that various behaviors followed other behaviors. Several differences between breast- and bottle feeding dyads revealed a tendency for the breastfeeding mothers to be more finely tuned to their infants' behaviors, and for the breastfeeding infants to exert greater control over the sequence of interactions. These differences are discussed in light of psychophysiological interdependency of breastfeeding couples. Developmental implications of the findings are discussed.

Introduction

Previous research has suggested that the mother-infant interactions which take place during the feeding episodes in the first few months of life may be crucial to the development of some of the infant's social and cognitive skills, such as reciprocal exchange in verbal communication, which is necessary for the acquisition of language. These early interactions may have an impact on many aspects of the infant's development, including his or her development of interpersonal relationships. It appears that the mother responds in synchrony with her infant, which teaches the sequencing of interpersonal behaviors which may be crucial to the child's later development of verbal communication (Schaffer, 1977). Dunn and Richards (1977) suggested that when an infant is allowed to play a part in the sequencing of interactions during feeding, and when its mother has timed her behavior in such a way that it is in rhythm with the baby's behavior, an important base for the development of synchrony and reciprocal exchange is formed.

This kind of reciprocity is a biological consequence of the physiological interdependence between breastfeeding mothers and infants. For example, infant suckling at the breast stimulates release of the hormones prolactin and oxytocin in the mother. These hormones stimulate the production of milk, and are associated with emotional reactions in the mother. After the first few days of breastfeeding, these physiological responses in the mother become conditioned to the behavior of the baby. The mother will come to secrete milk merely at the sound of her infant's cry. Because of this, the mother's own comfort is dependent on her bringing the baby to the breast. During each feeding episode as the infant varies the rate of sucking and alternates between nutritive and non-nutritive sucking, the mother will experience several milk ejection responses with their associated spikes in oxytocin levels, and with their associated effects on her emotional state.

Nature has designed a system which causes the breastfeeding mother to be finely tuned to her infant's behavior. Many similarities probably do exist between breastfeeding and bottle-feeding dyads at the psychological and socio-cultural levels of analysis; however, the fact that the breastfeeding mothers and their infants have a physiological interdependency which does not

†Lori is a senior psychology major from Benton, Ky.

exist in the bottle-feeding pairs, has led us to believe that there may actually be important differences between breastfeeding and bottle-feeding dyads in the sequencing of mother-infant

interactions during feeding episodes. This is in contrast to the widely accepted belief expressed by Schaffer (1977): "even during infancy itself, whatever the 'physical' advantages of breastfeeding, there are no distinctive psychological concomitants" (12).

Further work comparing breast- and bottle-feeding dyads needs to be done. Previous studies have inadequately defined breastfeeding and bottle-feeding. Breastfeeding mothers may have been supplementing with bottles, scheduling feedings, or engaging in other feeding practices that tend to disrupt the physiological interdependency of breastfeeding. Newton (1971) showed important differences between what she called 'token breastfeeders' and 'total breastfeeders'. These groups were apparently combined in most previous research. Also lacking in previous studies has been precision in the consideration of the sequencing and timing of interactions during feeding episodes.

Procedures

The goal of this research was to do a rigorous descriptive analysis of mother-infant interactions during feeding episodes, comparing the sequencing of behaviors in breastfeeding and bottle-feeding couples. Twelve mothers were videotaped during a feeding session with their 6- to 13-week-old firstborn infants. Half of the mothers were breastfeeders who had never supplemented with artificial feedings; the other half had never breastfed.[1] Each session was coded by two observers using event recording software Simonson (1985), which allowed for several passes to be made through the data, noting the beginning and ending times for each of 8 maternal and 7 infant behaviors. Disagreements between the coders in the identification or sequencing of events were resolved by reviewing the videotapes. Discrete behaviors, such as sucks, were divided into bouts with any 2-second pause delineating the boundaries between bouts. The starts and stops of the following fifteen behaviors were coded.

1. Baby sucks - the opening and closing of the infant's jaw, while on nipple.

2. Mother offer nipple - any movement instigated by the mother which brings the nipple and the infant's mouth within close proximity to one another.

3. Mother remove nipple - mother takes nipple out of infant's mouth.

4. Baby take nipple - infant grasps nipple in its mouth.

5. Baby refuse nipple - infant does not grasp nipple in mouth when presented or releases nipple after sucking.

6. Mother caress - any motion of the mother's hand on the infant's body (patting, rubbing, fingering).

7. Mother touch - still contact of the mother's hand on the infant not including the holding touch.

8. Baby caress - any motion of the infant's hands on any object (patting, rubbing, fingering).

---

[1] Additional data were collected with breastfeeding mothers who used supplemental bottle feedings and with bottle feeders who had initially breastfed.

9. Baby grasp - still contact of the infant's hand on any object, including grasping behaviors.

10. Mother vocalize - any mother vocalization directed at the infant.

11. Baby vocalize - any infant vocalization other than crying.

12. Baby cry - vocalizations of the infant that indicate negative affect.

13. Mother jiggle - shaking or bouncing of the infant of bottle in an up and down motion.

14. Mother rock - mother moving the infant in a side to side motion.

15. Reposition of the infant - mother changes the position of the infant's body.

Results and Discussion

A fifteen by fifteen transition matrix was constructed for each group indicating for each behavior, the probability that it was followed by any other behavior. Examination of the transitional probabilities led to a clustering of those behaviors that were similarly distributed. Figures 1 and 2 present models of the patterns of interaction observed among bottle- and breastfeeders respectively, while Table 1 represents the transitional probabilities of all combinations of any maternal and infant behaviors following one another.

An examination of Figures 1 and 2, and Table 1 reveal some interesting differences between breast and bottle-feeders. Maternal behaviors in the breastfeeding couples were more often responses to infant behaviors than they were responses to other maternal behaviors. The bottle-feeders tended to produce more strings of maternal behaviors. Among breastfeeders, the probability that one maternal behavior followed another maternal behavior was .18, while the probability that a maternal behavior followed an infant behavior was .22. Similarly, the probability of an infant behavior following a maternal behavior was .22, while the probability of breastfeeding infants following their own behavior was .38. For the bottle-feeders the pattern was different. The probability that a maternal behavior followed another maternal behavior was .43, while the probability that infant behavior followed another infant behavior was .11. The probability of maternal behavior following infant behavior and the probability of infant behavior following maternal behavior were similar to those of the breastfeeders, .23 and .22, respectively.

Breastfeeding mother's behaviors made up 40% of the total behaviors within the feeding episode, leaving 60% of the behaviors in the episode to be made by the infants. In contrast, the bottle-feeding mother's behaviors made up 66% of the total behaviors in the episode, leaving 34% of the behaviors to be made by the infant.

Other differences can be seen when referring to Figures 1 and 2. In these figures the relative frequency of the various categories of maternal and infant behaviors are represented by circle size. Bottle-feeding mothers vocalized much more frequently than did breastfeeding mothers, and there was a .37 probability that a maternal vocalization would be followed by another maternal vocalization. Infant suckling was more clearly responsive to maternal behaviors in the breastfeeders than in the bottle-feeders. For example, there was a .43 probability that a maternal tactile behavior would lead to a sucking behavior for breastfeeders, and a .20 probability for bottle-feeders.

Breastfeeding infant sucking behaviors also made up a larger proportion of the total

number of behaviors within the feeding episode than did bottle-feeding infant sucking behaviors. Differences were also found in the infant's nipple behaviors. Breastfeeding infants refused or spit out the nipple a mean of 6 times during the feeding episode. The bottle-feeding infants never refused or spit out the nipple (X = 0). On the other hand, whenever the nipple was out of the infant's mouth during the bottle-feeding episode (which occurred only 5 times across all the bottle-feeding pairs), the mother had removed the nipple from the infant's mouth. Removing the nipple from the infant's mouth occurred only once among breastfeeders. A X^2 test comparing breastfeeders to bottle-feeders on all four types of nipple behaviors coded (remove nipple, take nipple, refuse nipple, offer nipple), indicated significant differences,
X^2 (3) = 21.9, p < .001.urity in his/her attachment situation. Thus, when the infant goes out to explore the world, s/he already has a sense of his/her behavior effecting the environment and may be more secure in acting upon that environment.

In accordance with the findings of this study, the breastfeeding infant may have a head-start in the acquisition of strong bases for future social and cognitive development by virtue of interaction differences between breast- and bottle-feeding mother-infant dyads during feeding episodes. Further research into the feeding interaction needs to be conducted, however. The present study does little to shed light on the important aspects of the synchronization and timing of mother and infant behaviors within the feeding episode, an area that is little understood. A careful examination of the relative frequency of different sequences of behavior may reveal a system of implicit rules that govern the mother-infant interaction - rules that may be similar in structure to the primitive grammars the child will later acquire. These rules may differ for breast- and bottle-feeding pairs. This type of study may lead to a better understanding of the early feeding interaction as well as its importance in later social and cognitive development, particularly in the area of language development.

Acknowledgments

I would like to thank the members of the 1988 Research in Developmental Psychology class for their help in the collecting and coding of some of the data for this study. I would also like to thank Dr. Marsha Walton for her effort, guidance, and devotion in the doing of this research.

Literature Cited

Bateson, Mary Catherine. (1975). Mother-Infant Exchanges: The Epigenesis of Conversational Interaction. *Annal of New York Academy of Sciences*, 101-113.

Dunn, J.B. & Richards, M.P.M. (1977). Observations on the developing relationship between mother and baby in the neonatal period. In H.R. Schaffer (Ed.) *Studies in Mother-Infant Interaction.* London: Academic Press, Incorporated.

Kopp, Claire B. & Krakow, Joanne B. (1982). *The Child*. Massachusetts: Addison-Wesley Publishing Company.

Newton, Niles. (1955). *Maternal Emotions*. New York: Paul B. Hoeber, Incorporated.

Newton, Niles. (1971). Psychological differences between breast and bottle feeding. *The American Journal of Clinical Nutrition, 24*, 993-1004.

Piaget, Jean. (1952). *The Origins of Intelligence in Children*. New York: International Universities Press.

Schaffer, H.R. (1977). *Studies in Mother-Infant Interaction*. London: Academic Press, Incorporated.

Table 1

Transitional Probabilities for All Mother and Infant Move t to Move t+1 Behaviors

Move t to Move t+1 Combination	Breastfed	Bottle-fed
Mother - Mother	.18	.43
Infant - Infant	.38	.11
Mother - Infant	.22	.22
Infant - Mother	.22	.23

Note. The transitional probabilities included in this table are probabilities between any type of N behavior and any type of N + 1 behavior, classified only as mother or infant.

Figure 1

TRANSITIONAL PROBABILITIES FOR MOTHER-INFANT INTERACTION DURING BOTTLE FEEDING

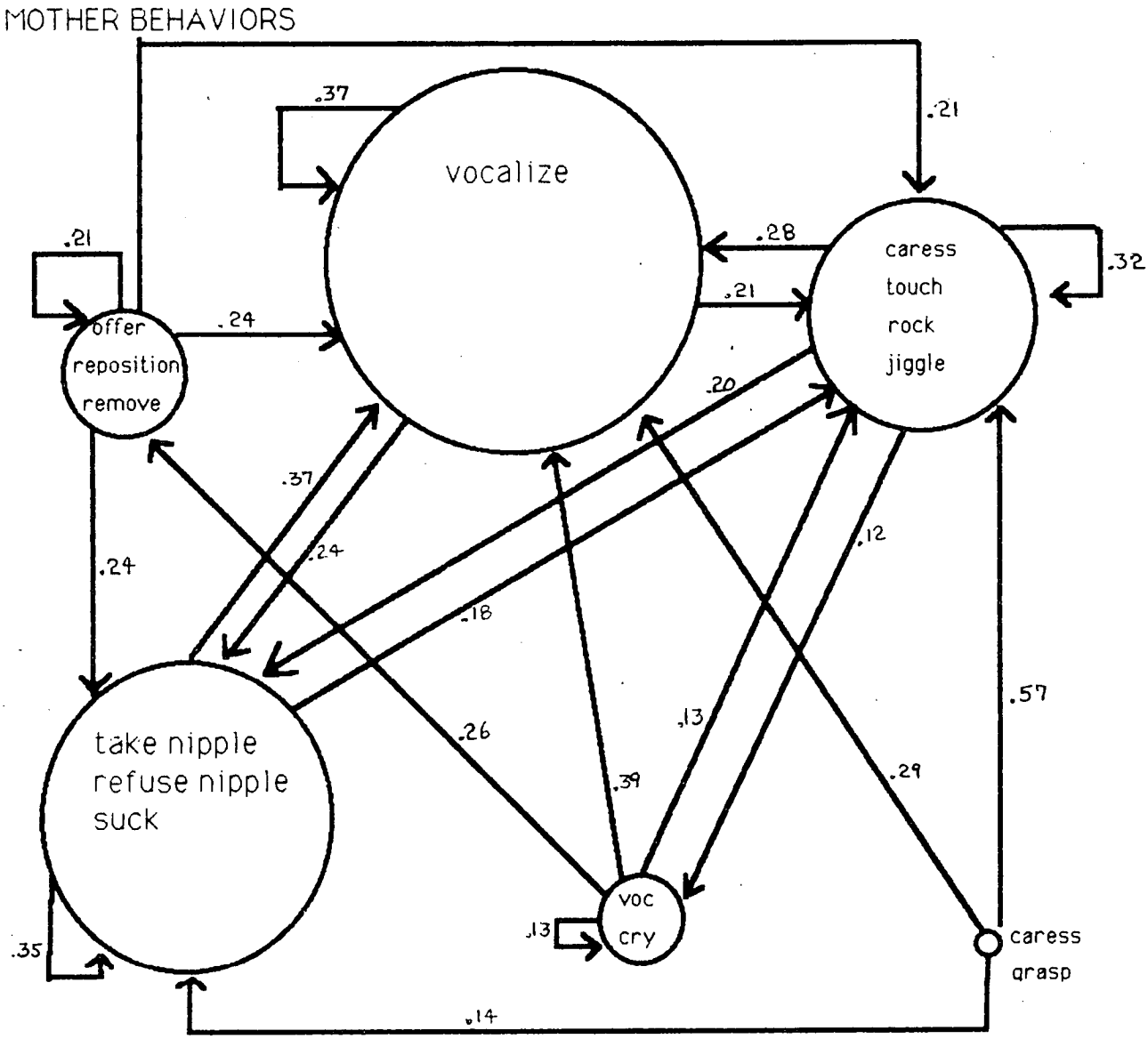

Note. This model describes 88% of the move n to move n+1 transitions for six mother-infant dyads. Nine additional arrows, each with a probability less than .10 would be required to account for the remaining data.

Relative frequency of the various categories of behaviors is represented by circle size.

Figure 2

TRANSITIONAL PROBABILITIES FOR MOTHER-INFANT INTERACTION DURING BREASTFEEDING

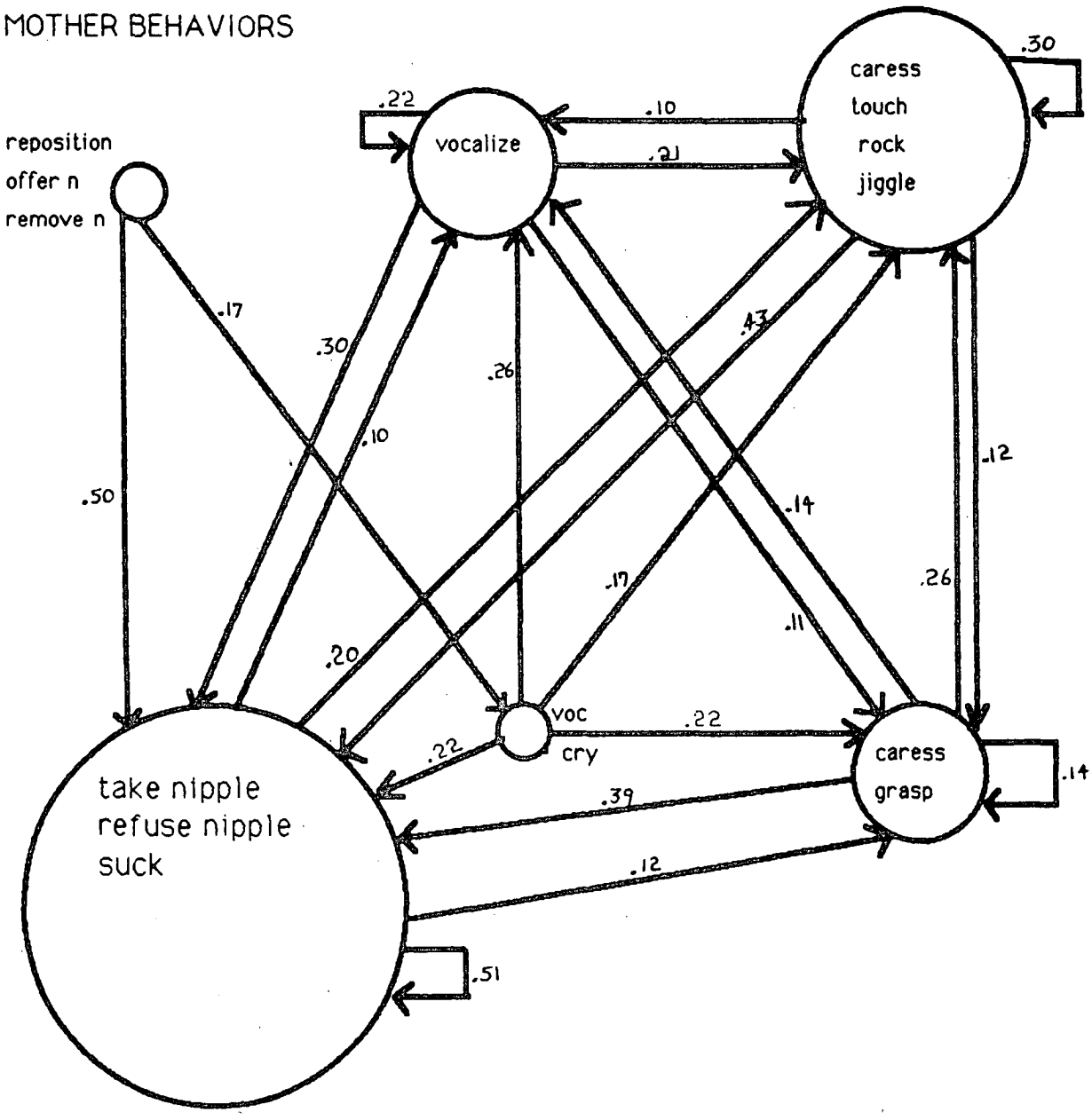

Note. This model describes 91% of the move n to n+1 transitions for six mother-infant dyads. Fourteen additional arrows, each with a probability less than .10 would be required to account for the remaining data.

Relative frequency of the various categories of behaviors is represented by circle size.

The Number of Self-Inverses in $\mathbb{Z}_n$

Cathy Robertson †

Abstract

*A self-inverse is a number n such that n is its own multiplicative inverse;i.e., n*n=1. The pattern involves n's unique prime factorization as $p_1^{k_1}p_2^{k_2}...p_j^{k_j}$ where the p_i are primes and the k_i are nonnegative integers. In this paper, a pattern for the number of self-inverses in the integers mod n is stated and proved.*

Introduction

If x and y are integers, we say that x is congruent to y mod n (written $x \equiv y \bmod n$) if x - y is divisible by n. For example, $4 \equiv 1 \bmod 3$ because 4 - 1 is divisible by 3. The integers mod n, $\mathbb{Z}_n$, is the set of all possible remainders when an integer is divided by n. For instance, if n = 3, $\mathbb{Z}_3$ = {0,1,2}.

Now, if a number x in $\mathbb{Z}_n$ has a multiplicative inverse in $\mathbb{Z}_n$, that inverse will be a number x^{-1} such that $x\,x^{-1} \equiv 1 \bmod n$. We know that the only numbers which have multiplicative inverses in $\mathbb{Z}_n$ are those that are relatively prime to n. Of those numbers, some are self-inverses; in other words, $x = x^{-1}$. For example, in $\mathbb{Z}_3$, 2 is its own inverse, because $2 * 2 = 4 \equiv 1 \bmod 3$.

I claim that there is a pattern to the number of self-inverses in $\mathbb{Z}_n$, and this pattern involves the prime factorization of n.

We know that n has a unique prime factorization as $p_1^{k_1} p_2^{k_2}...p_j^{k_j}$ where $p_1, p_2,..., p_j$ are primes and $k_i \geq 0$ for $1 \leq i \leq j$; as an example, consider the number 140. Its prime factorization is $2^2 * 5 * 7$.

Now, since 2 is a prime, we can write the prime factorization as

$$n = 2^m p_1^{k_1}... p_j^{k_j}$$

where $p_1,..., p_j, k_1,..., k_j$ are as above, and $m \geq 0$.

Main Result

Let C be the number of self-inverses in $\mathbb{Z}_n$. Then

$$C = \begin{cases} 2^0 * 2^j & \text{if } m = 0 \text{ or } m = 1 \\ 2^1 * 2^j & \text{if } m = 2 \\ 2^2 * 2^j & \text{if } m \geq 3, \end{cases}$$

where m and j are as above.

As an example, consider $\mathbb{Z}_{16}$. We know that the prime factorization of 16 is simply 2^4. So $m = 4 \geq 3$, and therefore, there are $2^2 = 4$ self-inverses in $\mathbb{Z}_{16}$; they are 1, 7, 9, and 15.

The proof of this result involves the Chinese Remainder Theorem, which is as follows: Let $p_1,..., p_m$ be relatively prime, and suppose

$x \equiv b1 \bmod p1$

$x \equiv b2 \bmod p2$

:

:

$x \equiv bm \bmod pm$

Then there is a unique solution to

$x \equiv a \bmod (p1\ p2 \ldots pm)$.

For instance, consider x = 11. Let p1 = 2 and p2 = 5; note that 2 and 5 are relatively prime. Then $11 \equiv 1 \bmod 2$ and $11 \equiv 1 \bmod 5$. Thus, we have a set of two congruencies, and, by theorem, there is a unique solution to the congruency $11 \equiv a \bmod (2 * 5)$. That solution is a = 1.

We can now begin the proof of the result.

First, recall that n has a unique prime factorization as $2^m\ p1^{k}1 \ldots pj^{k}j$. To find the number of self-inverses in $\mathbb{Z}n$, we must find the number of solutions to $x^2 \equiv 1 \bmod n$.

We know that if $x^2 \equiv 1 \bmod n$, then, where each pi is an odd prime (i.e., $pi \neq 2$),

$x^2 \equiv 1 \bmod p1^{k}1$

$x^2 \equiv 1 \bmod p2^{k}2$

:

:

$x^2 \equiv 1 \bmod pj^{k}j$.

Claim: There are two and only two solutions to each of these congruencies, namely 1 and $(pi^{k}i - 1)$ for $1 \leq i \leq j$.

To see this, let p be an odd prime and suppose $x^2 \equiv 1 \bmod p^k$. Then p^k must divide evenly into $(x^2 - 1) = (x + 1)(x - 1)$. Since p obviously divides evenly into p^k, p must divide evenly into $(x + 1)(x - 1)$. Then p must divide evenly into at least one of (x + 1) and (x - 1).

Suppose p divides evenly into (x + 1). Then p cannot divide evenly into (x - 1), since the difference between (x + 1) and (x - 1) is 2, and p > 2. But if p does not divide evenly into (x - 1), obviously p^k cannot divide evenly into (x - 1). Therefore, p^k must divide evenly into (x + 1); in other words, $x \equiv -1 \bmod p^k$. So x must be $(p^k - 1)$.

On the other hand, if p divides evenly into (x - 1), then p cannot divide evenly into (x + 1), so p^k cannot divide evenly into (x + 1). Therefore, p^k must divide evenly into (x - 1); in other words, $x \equiv 1 \bmod p^k$, so x = 1.

Thus, if p is an odd prime, the only solutions to $x^2 \equiv 1 \bmod p^k$, are 1 and $(p^k - 1)$.

Now, by the Chinese Remainder Theorem, we know that for each solution to the congruencies

$x^2 \equiv 1 \bmod p1^{k}1$

$x^2 \equiv 1 \bmod p2^{k}2$

:

:

$x^2 \equiv 1 \bmod pj^{k}j$,

there is a unique solution to the congruency $x^2 \equiv 1 \bmod (p_1^{k_1} \ldots p_j^{k_j})$. Since there are two and only two solutions to each of the congruencies $x^2 \equiv 1 \bmod p_i^{k_i}$, and since we have j such congruencies, there are 2^j solutions to $x^2 \equiv 1 \bmod (p_1^{k_1} \ldots p_j^{k_j})$, as claimed.

Thus, we have shown that for each prime other than 2 in the prime factorization of n, there are two self-inverses in $\mathbb{Z}_n$.

Now, consider the 2^m in the prime factorization of n. We know that if $x^2 \equiv 1 \bmod n$, then it must be true that $x^2 \equiv 1 \bmod 2^m$. Hence 2^m divides evenly into $(x^2 - 1) = (x + 1)(x - 1)$. We know that since 2^m is even, both $(x + 1)$ and $(x - 1)$ must be even.

Let z be either $x + 1$ or $x - 1$, and, without loss of generality, suppose 4 divides evenly into z. Then 4 cannot divide evenly into the other factor, so the other factor must be 2q, where q is odd.

Then $(x + 1)(x - 1) = z * 2q$, so 2^m must divide evenly into 2zq; in other words, 2^{m-1} divides evenly into zq. But since q is odd, we know 2^{m-1} must divide evenly into z.
Therefore, either $z \equiv 0 \bmod 2^m$ or $z \equiv 2^{m-1} \bmod 2^m$.

This gives us four solutions. Consider $z = (x - 1)$:

1) If $(x - 1) \equiv 0 \bmod 2^m$, then $x \equiv 1 \bmod 2^m$, so $x = 1$.
2) If $(x - 1) \equiv 2^{m-1} \bmod 2^m$, then $x \equiv (2^{m-1} + 1) \bmod 2^m$, so $x = (2^{m-1} + 1)$. Now, consider $z = (x + 1)$:
3) If $(x + 1) \equiv 0 \bmod 2^m$, then $x \equiv -1 \bmod 2^m$, so $x = (2^m - 1)$.
4) If $(x + 1) \equiv 2^{m-1} \bmod 2^m$, then $x \equiv (2^m - 1) \bmod 2^m$, so $x = 2^{m-1} - 1$.

We want to check that each of these four solutions really satisfies $x^2 \equiv 1 \bmod 2^m$:

1) Obviously, $x = 1$ satisfies $x^2 \equiv 1 \bmod 2^m$.
2) Suppose $x = 2^{m-1} + 1$. Then $x^2 = (2^{m-1} + 1)^2 = 2^{2m-2} + 2^m + 1$, and since 2^m divides evenly into 2^{2m-2} and 2^m, we know $x^2 \equiv 1 \bmod 2^m$.
3) Suppose $x = 2^m - 1$. Then $x^2 = (2^m - 1)^2 = (2^{2m} - 2^{m+1} + 1) \equiv 1 \bmod 2^m$.
4) Suppose $x = 2^{m-1} - 1$. Then $x^2 = (2^{m-1} - 1)^2 = (2^{2m-2} - 2^m + 1) \equiv 1 \bmod 2^m$.

Thus, each of the four solutions $1, 2^{m-1} + 1, 2^m - 1, 2^{m-1} - 1$ satisfies $x^2 \equiv 1 \bmod 2^m$.

Note that if $m = 2$, then $2^{m-1} + 1 = 2^m - 1$, and $1 = 2^{m-1} - 1$, so there are actually only two solutions.

If $m = 0$ or $m = 1$, then we obviously only get one solution to $x^2 \equiv \bmod 2^m$, that is, $x = 1$.

Therefore, the congruency $x^2 \equiv 1 \bmod 2^m$ has the following number of solutions: If $m = 0$ or $m = 1$, there are $1 = 2^0$ solutions. If $m = 2$, there are $2 = 2^1$ solutions. Finally, if $m \geq 3$, there are $4 = 2^2$ solutions.

Thus, as claimed, the number of self-inverses in $\mathbb{Z}_n$ where $n = 2^m p_1^{k_1} \ldots p_j^{k_j}$ is

$$C = \begin{cases} 2^0 * 2^j & \text{if } m = 0 \text{ or } m = 1 \\ 2^1 * 2^j & \text{if } m = 2 \\ 2^2 * 2^j & \text{if } m \geq 3. \end{cases}$$

The Effects of White, Red and Blue Light on Three Movement Behaviors in Daphnia

Kenneth M. Cameron†

Abstract

Daphnia were observed by students under White, Red, and Blue light conditions in the laboratory for a total time of three minutes per light color. Movements were defined and recorded by each student and tested for significant difference using the Chi-Squared test. The animals exhibited the greatest amount of horizontal swimming under blue light and the greatest amount of vertical orientation under red light, with white producing an intermediate effect. Animals were more active under conditions of red light, followed by white light, and showed the lowest activity under blue light. Animals were found to be positively phototrophic under white light, less so under red, and much less so under blue. Explanations as to the adaptive significance of these behaviors are best explained by theories of feeding efficiency, predator avoidance ,and harmful light avoidance .

Introduction

Members of the genus Daphnia, more commonly known as water fleas, are small freshwater invertebrates of the order Cladocera. Because of their interesting shape and behavior, they have been a favorite laboratory subject for years. In particular, they have been popular in experiments dealing with the effects of light on invertebrate behavior(Pennak 1978).

It has been well documented that many invertebrates, including Daphnia, exhibit a diurnal pattern of vertical migration. Through careful manipulation of conditions, light intensity has been found to be the primary driving force in this phenomenon. Daphnia tend to migrate to the surface of a body of water during night hours and descend to lower depths during daylight, this pattern is reversed, however, in several species (Gauthreaux 1980). Timing of diapause has also been found to correllate with light intensity. In addition, a circadian rhythm for activity has been discovered, with Daphnia being most active during the day hours and much less so during the night (Stearnes 1975). Thus, there exist several interesting effects of light intensity on behavior patterns in Daphnia. More interesting, perhaps , are the studied effects of light color (wavelength) on these organisms.

In 1953, Smith and Baylor noticed that Daphnia behaved very differently under conditions of Red or of Blue light than they did under normal white light exposure. They found that under Red light (735 nm) Daphnia tended to dance upright in the water along a vertical plane and appeared very calm. They called this the "Red Dance". In Blue light, however, the Daphnia appeared very agitated, moving frantically along a horizontal vector. They termed this response the "Blue Dance" and noted that populations have been seen to be driven to death under this condition. In normal White light, Daphnia seem to perform a combination of the two dances described above or switch from one to the other at random. While Smith and Baylor also uncovered some amazing relationships between temperature , intensity of light, and effect of polarized light on Daphnia, it is their results with light color that have been the most fascinating yet most puzzling of all (Smith and Baylor 1953).

To explain the observed color dances of these and other similar creatures, researchers have proposed several theories. The most commonly held proposes that Daphnia move differently under conditions of different light wavelength in order to maximize their feeding strategies (Smith and Baylor 1953). Some feel that harmful effects of high frequency light causes migration away from

†Ken is a senior Biology major from Murfreesboro, TN.

the source, while still others discuss the avoidance of predators or a combination of all of these as factors that come into play (Hairston 1976,1979, 1981) . While Daphnia do possess an eye-like photoreceptor, experiments with blinded individuals yield the same results, suggesting that, more importantly than eyes, dermatoptic senses play a part in light induced taxes (Carthy 1968).

The purpose of this experiment was to observe Daphnia under Red , White, and Blue light to demonstrate the effects of the three wavelenghts on the individuals as has been reported, and to present some theoretical explanations for these observations .

Procedures

Approximately twenty individuals of an unidentified Daphnia species of various sizes and ages were kept at constant temperature, pH, and white light intensity in two ten gallon aquaria. Except for some organic material settled on the bottom of the tank, there were no refugia for the organisms. The water in the tank was free of particulate matter and appeared clear.

Between the hours of 1:00 and 5:00 pm on September 1, 1988, each student observed a single individual of Daphnia under the effects of white, red and blue light for exactly three minutes per light color. The light source was of a flourescent nature and was directed from above the aquarium. To achieve the appropriate light wavelengths for the experiment, red and blue colored plastic filters were positioned between the white light source and the aquarium.

The instructions for the experiment were simply to observe the Daphnia, define a movement, quantify the movement under the three light conditions, and analyze the collected data by using the Chi-squared test where

$$X^2 = \frac{(\text{observed} - \text{expected})^2}{\text{expected}}$$

and the null hypothesis was that there is no difference in movement of the Daphnia under the three wavelenghths of light (Kesler 1988).

Results

Class discussion following the experiment indicated that, except for a few questionable results, the null hypothesis for the experiment was rejected by nearly all. Results available for this report were limited to those of only eight students of the fourteen in the class who submitted results, but these results seem to correlate well to the results presented in the above mentioned discussion. Because of the open-ended aspect of the experiment, measured movement of the Daphnia under observation was not the same for each student. Nevertheless, there was some overlap, with quantified movement falling into one of three categories: movement horizontally/vertically, total movement, or movement toward/away from the light source. The results can be found in Data sets 1, 2, and 3.

Data Set 1

HORIZONTAL/VERTICAL

#1 observed number of horizontal jerks less than 45 degrees and number of vertical jerks more than 45 degrees

	Vertical	Horizontal
White	67	107
Red	190	70
Blue	65	133

X^2=95.5, degrees of freedom=2, $p < .05$
Conclusion: Reject the null hypothesis

#2 observes total jumps, but indicates general direction (see next page as well)

White	Half Vertical, Half Horizontal
Red	Generally Vertical
Blue	Generally Horizontal

Data Set 2

TOTAL MOVEMENT

#2 Observed total number of jumps in any direction excluding falling action (see previous page as well)

White	114
Red	153
Blue	87

X^2=18.6, degrees of freedom=2, $p < .05$
Conclusion: Reject the null hypothesis

#3 Observed total of 0.5 cm jumps

White	80
Red	86
Blue	60

X^2=4.89, degrees of freedom=2, $p < .05$
Conclusion: Accept the null hypothesis

#4 Observed total movement horizontally + vertically

White	62
Red	82
Blue	39

X^2=15.1, degrees of freedom=2, $p < .05$
Conclusion: Reject the null hypothesis

Data Set 3

MOVEMENT TOWARD/AWAY FROM THE LIGHT

#5 Observed time spent "jumping upward"

White	100 sec/3 min
Red	83 sec/3 min
Blue	58 sec/3 min

X^2=11.1, degrees of freedom=2, $p < .05$
Conclusion: Reject the null hypothesis

#6 Observed time spent going up

White	92 sec/3 min
Red	79 sec/3 min
Blue	39 sec/3 min

X^2=21.8, degrees of freedom=2, $p < .05$
Conclusion: Reject the null hypothesis

#7 Observed number of times touched down on bottom

White	26
Red	15
Blue	10

X^2=7.9, degrees of freedom=2, $p < .05$
Conclusion: Reject the null hypothesis

Discussion

The results of this experiment correlate in most instances with the results found by past researchers. Daphnia exhibit the behavior of Blue and Red Dances as described in the classic study by Smith and Baylor, and also show a tendency to be more active in red light, least active in blue, positively phototropic to white light and negatively phototropic to blue.

Before proceeding with a discussion on the adaptive value or explanations of these observed phenomena, several causes of possible error and/or bias must be addressed. In comparing the results of this experiment with the results of others, it must be emphasized that behavior patterns among all Daphnia species is not the same. The Daphnia used in these tests were not identified. Moreover, regardless of species, the individuals used were most likely clones that would not exhibit the range of variable behavior found in nature. Hence, comparisons should be treated as general.

The age of the individuals tested was also neglected in these tests, as was time of day, specific pH, specific temperature, intensity of the light source, and time of feeding. According to Huthinson (1967), G.L. Clarke found that very young animals were far more positively phototropic than mature animals. Stearnes showed that Daphnia exhibit a circadian rhythm of activity and that within this rhythym, the amount of horizontal and vertical movement changed with time (Stearnes 1975). The factor of unknown pH is also relevant. Daphnia magna reared at pH 8.0 becomes strongly positively phototropic at pH 8.5, and negatively so at pH 7.0 (Huthinson 1967) indicating that a bias could have entered into our experiment in this context. While the Daphnia culture used in the experiments was kept at uniform room temperature, extreme changes of temperature have been reported to alter the dancing behavior of Daphnia as have differences in

light intensity (Smith and Baylor 1953). The light source was kept at a constant intensity, but scattering of light by the colored filters undoubtedly biased the intensity received to the animals in the white light.

The type food and time of feeding may also have introduced an error factor into the experiment. Daphnia fed on algae are more positively phototropic than those fed on bacteria (Huthinson 1967). In addition, Daphnia tend to move more horizontally when hungry and vertically during and after feeding (Stearnes 1975).

Finally, errors in timing, following a single individual for a three minute time period, bias toward large or small individuals and other such personal errors play a role in shaping the results of such a study.

Horizontal/Vertical Movement

The Red and Blue dances observed originally by Smith and Baylor (1953) and recreated in this experiment present an interesting puzzle for the animal behaviorist. To explain the tendency for Cladocera to move along a horizontal in Blue light and along a vertical vector in Red light, researchers have turned to feeding strategy. A theory held for quite some time proposes that Daphnia swimming in a body of water seek out patches of phytoplankton in which to feed. The light beneath a patch of phytoplankton is of low wavelength (red) because phytoplankton tend to reflect higher wavelength light (blue) when they cluster. A Daphnia that has located a patch of algae and is positioned beneath or within it, benefits by keeping its movements in one place along a vertical vector. On the other hand, a Daphnia is at an advantage to swim quickly along a horizontal vector when it encounters blue light since light of this wavelength would tend to correlate with open, algae poor water (Smith and Baylor 1953).

Those in opposition to this theory state that there is no evidence that algae tend to clump near the surface of lakes, and that even if they did, Daphnia have been shown to be less efficient feeders when the density of phytoplankton increases above 1.5 mg of phytoplankton/L of water and thus, would tend to swim away from high concentrations of algae toward clearer water (Bliss 1983). Moreover, it is argued that because blue light penetrates into deeper water than red light, enough high wavelength light would reach Daphnia beneath algal clusters to cancel the effects of increased red light. Dissolved and particulate matter are also known to shift the spectrum of light in water toward the red. According to Stearnes, if Daphnia were relying on spectral differences to find their food, they would involve themselves in "fruitless activity" , roaming away from algae in turbid waters and keeping station in acid stained, algae free water (Stearnes 1975).

Total Movements

The results of this experiment show that Daphnia are most active under conditions of red light than they are under conditions of blue, with white being intermediate. Studies of copepods with and without red pigments show that the organisms without red pigmentation tend to move much slower in blue light than in red and much slower under all wavelengths than pigmented copepods. While this seems contradictory to the results reported here, there may be an explanation. To explain what was seen with the Codepods, Hairston suggested that pigmented copepods were at an advantage to swim quickly in order to avoid predators that hunted by sight, yet he also presents the idea that slower swimming may be just as advantageous because it makes an organisms less obvious to the predator Hairston 1976 and 1979).

The problem lies in whether faster of slower swimming is most advantageous to a Daphnia under blue light. Consider an individual Daphnia just having fed on Algae, its primary food source. Because the carapace of most Daphnia is clear, the individual might take on a blue/green color because of algal cells within its intestine. If this is the case, and swimming slowly is more advantageous in avoiding predators as has been suggested, then the Daphnia should be expected to swim more slowly and hence be less active in Blue light as we have seen.

In his study on circadian activity rhythms of Daphnia, Stearnes reports that Daphnia are most active during the daylight hours and that during these hours, vertical movement (as characterized under Red Light) is the predominate directional movement. He explains this in terms of feeding time of the animals. Daphnia reach their peak feeding time during these

daylight hours when spectral stimuli are available to locate food items, if one assumes that the two are related. If, in some way, blue light mimics darkness , or our blue filters decreased the light intensity to mimic darkness we would expect to see the decrease in activity under blue light as we did.

Finally, while Smith and Baylor's observation that fast agitated action occurs under blue light and calm movement occurs under red seems to contradict our findings as presented here, they and several others have shown that exposure to harmful long wavelenghts of light weakens Daphnia and other aquatic invertebrates to the point of a substantially increased mortality rate (Smith and Baylor 1953, Hairston 1976,1981). Perhaps this explains the observed lower activity of our Daphnia under Blue light.

Rising/Falling Movements

The final tendency observed for the Daphnia in this set of experiments is a significant upward movement of the animals under white and red light opposed to blue light. One student reported that under conditions of blue light, the Daphnia were observed to touch the bottom of the aquarium a more significant number of times than they did under the other colors. Many theories have been given to explain this phenomenon. The most plausible has to do with the deleterious effects of blue light on Daphnia and other freshwater invertebrates as mentioned previously. Since high energy light (Blue) penetrates to a deeper depth than safe red or white light, Daphnia benefit by moving downward to deeper water layers under high exposure to blue light.

If, as mentioned previously, darker blue light mimics night darkness, then the observation of positive phototropism to white and red light is contradictory to what is actually seen in nature. Daphnia exhibit a diurnal vertical migration like many other aquatic zooplankton, rising toward the surface during the night hours in order to feed and to avoid predators, especially fish which often cannot see the Daphnia at night (Gauthereaux 1980).

A final hypothesis to explain this increased photo taxis toward white light is that particular food sources in the aquarium are either reacting toward the change in light intensity or color or that the Daphnia are able to see particular food sources under the different colors . Phytoplankton are known to have a vertical migration pattern opposite to most Daphnia species. If phytoplankton in the aqaurium are responding to the light changes and descending with blue light, then the Daphnia may follow them to reach optimal feeding depths. Likewise, if a food source that is more visible under red light is situated toward the surface waters and another that is more visible under blue light is situated near the bottom, the Daphnia may adjust to optimal depths as well.

Conclusion

While the results of this experiment support the findings of Smith and Baylor, they also present some discepancies. Blue and Red Dances are best described as related to feeding efficiency, although more and more evidence seems to be favoring an alternative hypothesis such as avoidance of harmful high energy light waves. Predation is undoubtedly the driving force behind increased/decreased activity under different light conditions, but several other hypotheses have been suggested. Vertical migration is accounted for by harmful light avoidance, predator pressures, and feeding strategy in most animals under natural conditions. The results of these experiments bring up other thoughts about migration and orientation in Daphnia under artificial wavelengths of different energy that are somewhat puzzling but certainly interesting.

Literature Cited

Baylor, Edward R. and Smith, Frederick E. (1953) "The Orientation of Cladocera to Polorized light," *American Naturalist, 87*:97-101.

Carthy, J. D. and Newell, G. E., (1968) *Invertebrate Receptors*, Academic Press, London.

Fogg, G. E., (1975) *Algal Cultures and Phytoplankton Ecology*, The University of Wisconsin Press, Madison.

Gauthreaux, Sidney A. Jr., (1980) *Animal Migration, Orientation, and Navigation*, Academic Press, New York.

Hairston, Nelson G. Jr., (1976) " Photoprotection by carotenoid pigments in the copepod Diaptomus nevadensis," *Proc. Nat. Acad. Sci. USA*, 73(3):971-974

---------- (1979) "The Adaptive Significance of Color Polymorphism in Two Species of Diaptomus (Copepoda)," *Limnology and Oceanography, 24*(1):15-37.

---------- (1981) "The Interaction of Salinity, Predators, Light and Copepod Color," *Hydrobiologia, 81*:151-158.

Hutchinson, G. E., (1957) *A Treatise on Limnology v. 1*, John Wiley and Sons, New York.

---------- (1967) A Treatise on Limnology v. 2, John Wiley and Sons, New York.

Kesler, David H. (1988) "Taxes, Speed of Movement, Chi-Squared and Paired Student's t-Test," *Animal Behavior Bio 207.*

Pennak, Robert W., (1978) *Fresh-Water Invertebrates of the United States*, John Wiley and Sons, New York.

Smith, Frederick E. and Baylor, Edward R., (1953) "Color Responses in the Cladocera and Their Ecological Significance," *American Naturalist, 87*:49-55.

Stearns, Stephen C., (1975) "Light Responses of Daphnia pulex," *Limnology and Oceanography, 20*(4):564-570.

Vernberg, F. John and Vernberg, Winona B., (1983) *The Biology of Crustacea v. 8*, Academic Press, New York.

GAMMA DECAY OF THE DELTA RESONANCE

Jennifer Gaines†

Abstract

The Reaction Spectroscopy Group in Oak Ridge National Lab's Nuclear Physics Division hopes to perform an experiment to study the gamma decay of the delta resonance in a nuclear medium. This paper will focus on the feasibility study of this proposed experiment as explored through a computer simulation.

Introduction

Charge Exchange Reactions and the Delta Resonance

A charge exchange reaction occurs when two particles collide and the charge of the bombarding particle is changed. The probing particle is usually a proton or a nucleus of some sort. The target particle can either be an individual nucleon or an entire nucleus. Considering the case of a nucleus target, when the probe strikes the target, a particle with different charge can emerge. The nucleus has gained energy and can react in several ways. For small amounts of energy, there are numerous possible excited states corresponding to slight rearrangements of the nucleons. These states are called "particle hole states"(Roy-Stephan, 373c).

At a certain point, there is enough energy to boost an individual nucleon to its first excited state. This stage is called the "delta resonance". When a neutron is the excited particle the resonance is a delta^{+}; for a proton it is called a delta^{++}. It is assumed that the ratio of protons to neutrons is constant throughout the nucleus; thus, for ^{208}Pb it can be determined that 66% of the excitement should be to delta^{++} and 34% to delta^{+}.

The energy (mass) distribution of the delta resonance is a Breit-Wigner distribution centered at 1232 MeV with a full-width-half-maximum of 115 MeV. The amount of energy required for this resonance to occur equals the difference between the mass of the delta and the mass of the nucleon, that is, about 300 MeV.

There have been experiments showing delta resonances in free nucleons, and experimenters hope to study more delta resonances from nucleons bound within nuclei. The lighter a probing particle is, the deeper it can penetrate a nucleus to excite a nucleon. It is of great interest to study these delta resonances and note the effect of the nuclear medium in the differences from free nucleon delta resonances. Differences are expected because the quarks within nucleons more deeply inside the nucleus may be more likely to be affected by nearest neighbors than those at the surface of the nucleus.

Delta resonances can decay in many ways. In order to balance the charge, the delta^{++} must always emit a π^{+} and leave a proton. The delta^{+} can emit a π^{+} and leave a neutron, emit a π^{0} and leave a proton, or emit a single gamma ray and leave a proton. In

† Jennifer is a junior Physics major from Bristol, TN.

free nucleon delta resonances, some type of pion emission occurs 99.4% of the time, and single gamma ray emission only .6% of the time. All together there are 377 times more π^+ emissions and 112 times more π^0 emissions than single gamma ray emissions. Experimenters hope to measure the photon decay of the bound nucleon delta resonances and compare it with the .6% figure for free nucleons. This procedure has two fundamental parts: exciting the delta resonance and detecting the photon decay.

The Experiment in Question

There have been several experiments proposed to demonstrate excitation of the delta in bound nucleons. The experiment in question would use a ^{208}Pb nucleus as a target and a ^3He nucleus as a probe, set up a charge exchange reaction, excite the delta resonance and emit a triton (^3H). This trition would continue on and be intercepted by a sensitive magnetic spectrometer, which could determine its mass and energy. A graph of these energies shows a large peak, 300 MeV below the original energy; this peak points out the excitation of the delta resonance. Several clusters of detectors would be placed at different angles around the point of collision to detect the gamma rays from the decay.

The proposed detector configuration is a 19-pack of hexagonal Barium Fluoride (BaF2) detectors. BaF2 crystals are good scintillators and are also dense enough to provide the stopping power required when dealing with high energy gamma rays. Scintillators, in general, absorb radiation which reacts in many different ways: pair production (most common), Compton scattering, by the photo electric effect, and by producing bremstrahlung. While some of the energy escapes, a veritable shower of electrons with energy proportional to that of the striking radiation is created, causing tiny sparks of light. Attatched to the crystals would be sensitive photomultipliers which detect the light and electrically magnify it to a current which can be read easily; thus, the original amount of energy deposition at the crystal can be determined.

Why a Feasibility Study?

Single gamma decay from the delta resonance is an uncommon occurence, but this alone does not make the proposed experiment difficult. π^+ 's have long lifetimes (~25ns) and decay to muons and electrons. Furthermore, they create different pulse shapes in the BaF2 detectors than gamma rays; thus they should be easily distinguished. However, this is not the case with π^0 's. The π^0 's are very short-lived, (<<1 ns) and decay to two gamma rays, (one of which could have energy comparable to that of single gamma ray emission) creating a huge amount of background radiation which could obscure the desired spectrum.

Thus, experimenters felt a feasibility study was warranted. Such a study would simulate the proposed experiment, and once the data was taken it would gate on given parameters in an effort to create a distinguishable single gamma ray spectrum. Some of the most important of the gates involve discriminating against events in which both gamma rays from a single π^0 decay strike the same 19-pack. Since the minimum angle between the two gamma rays of a π^0 decay at the peak of the delta is known to be 60.9 (from the equation $\theta_{\gamma\gamma}^{min} = 2\sin^{-1} 1/\gamma\pi_0$, where $\gamma\pi_0 = E/m\pi$),(Stroher,568) the detectors can be positioned close enough to the point of collision that they would be likely to detect both gammas. Several different gates can be created to search for this factor. Other spectra can be gated precisely around chosen mass distributions, due to the measurement of triton masses by the spectrometer. The higher the triton mass, the lower the energy of the gammas a pions, and vice verse. Further studies can demonstrate that the spectra of π^+ emission should not interfere.

Procedures

The feasibility study conducted for this experiment was centered around a computer simulation of the experiment and involved three main steps: writing a working simulation of the experiment with appropriate geometrical properties of the desired setup, making multiple runs to build up statistics under different conditions, and writing a histogramming program to graph the energy deposition in the detectors under different gating parameters to determine if single gamma radiation is distinguishable from π^0 decay.

The computer simulation of this experiment was written using the series of GEANT codes developed by CERN. Within GEANT are many Monte Carlo routines written to very accurately simulate the response of a real detector system to all types of particles, including gamma rays and pions. The programmer's job was to write one composite FORTRAN program, choosing among the appropriate subroutines and manipulating them to suit the experiment under study.

One vital GEANT subroutine is UGEOM, in which the user defines the geometrical parameters of the setup. It includes subroutines for defining the sizes, shapes, positions, rotation matrices, and compositions of detectors. Since it is easy to position a group of sensitive detectors within a dummy volume of air, the simulation is efficient for moving things around the "laboratory" to try different setups. The interactive version of GEANT allows the user to draw the entire lab setup on the screen, to look at it from many angles and cross-sections, and even to trigger events and watch as the particles enter the detectors and create showers of other particles.

For this simulation, four types of volumes were defined. One large cube of air, designated "LABO" served as the "laboratory". Positioned within LABO was a large cylinder of air which was parent to nineteen copies of a hexagonal volume made of BaF_2. For a simplest case simulation, only one 19-pack was present, but the program was written such that the number of detectors could easily be expanded. The fourth volume type was a large slab of iron, used to represent the large amounts of iron present in an actual laboratory. Such material can scatter gamma rays into detectors when they are not originally heading for them. Simulations were performed both with and without this scattering element.

Another main section of GEANT is GUKINE in which the user defines all of the kinematics and launches each event. An event includes the release of a particle and tracking of it and all the subsequent radiation it creates within the detector. Proper particle types, energy and mass values, and momentum and angle of release are all calculated here, often using random number generators.

For this particular simulation, the Breit-Wigner shape of the delta resonance was not very efficient because of the long "tail" regions with nearly zero counts. Near the peak it can be approximated with a Gaussian shape, as was done in this case. In the first variation, a mass, RMASS, was selected randomly from the entire distribution. The gamma energy was defined as: RMASS - mass of nucleon (938 MeV); the pion energy was defined to be:

$$\frac{\text{RMASS} - (\text{mass of nucleon})^2 + (\text{mass of pion}(135\ \text{MeV}))^2}{2 * \text{RMASS}} - \text{mass of pion}$$

Angle of release values were chosen at random within pre-programmed boundaries. The momentum of the pion was defined to be: $(E^2 + 2 * \text{mass of pion})^{1/2}$. Later the RMASS was chosen to be a random number within a distribution 10 MeV wide centered at a given excitation energy.

After each event is completed, the program gives control to the subroutine GUSTEP which stores the detector numbers and energy depositions for the previous event. The final step occurs in the subroutine GUOUT which formally stores all the information in arrays developed by the programmer for easy interpretation in histogramming. The final programming task was to write a histogramming program to display the data.

Results

The first results from the entire mass distribution were very disappointing in that the pion gamma radiation completely masked the single gamma emission spectrum. Fortunately, after gating around specific excitation energies (200, 300, and 400 MeV) distinguishable, if faint, single gamma emission peaks began to appear.

Several different gating techniques were used to try to suppress the pion peak without suppressing the gamma peak, with varying degrees of success. These included gates on the number of detectors fired above a threshhold energy, the spatial difference between the greatest and second greatest energy deposition per hit, and others designed specifically to use the minimum angle factor.

Due to the load on the computer facilities at Oak Ridge, accumulating data and processing it into histograms became a very slow process. At summer's end, indications were that the experiment under consideration is feasible, but very difficult.

Conclusion

Experimenters wish to study the photon decay of the delta resonance in a nuclear medium in order to note the differences from that decay in free nucleons. Such an experiment warranted a feasibility study because of the large amount of background gamma radiation given off by the decay of π^0. This feasibility study was performed by writing a GEANT computer simulation. More simulated runs using the basic program are planned, but at this stage it appears that this experiment would be very difficult to perform.

Experimenters plan to continue the simulation using the programmer's basic groundwork. Scheduled runs include different detector positions, more detector clusters, greater granularity of detectors (more detectors per unit volume), and more and different gates on histogramming. These are all program variations which can be made simply.

Literature Cited

Roy-Stephan, M. *Nuclear Physics A482* (1988) 373c.

---------- Collective Excitations of Spin-Isospin Modes, journal and date unknown.

Stroher, H., et al. *Nuclear Instruments and Methods in Physics Research A269* (1988) 568.

Udagawa , T. and F. Osterfield *Nuclear Physics A482* (1988) 391c--404c.

Sequencing the Thrombospondin Promoter

Salil Parikh†

Abstract

The object of this project was to sequence a 1.7 kilobase strand of the promoter region of the thrombospondin gene. The Sanger Dideoxy method was employed for sequencing. This procedure involved cutting the DNA cosmid library to obtain the correct insert, placing the insert into a plasmid vector, injecting the vector with a phage, and subsequent sequencing of the DNA with a DNA polymerase using polyacrylamide gel electrophoresis. Sixteen hundred bases were sequenced. The goal of this sequencing study was to identify similarities of base pair sequences between the thrombospondin promoter and other known promoter regions to determine similar thrombospondin activation factors between the thrombospondin gene and other genes.

Introduction

Thrombospondin (TS) is a large, trimeric, modular protein that is found in the alpha granules of the paltelets and is secreted by various epithelial cells. Because TS is released during platelet activation and is bound to the platelet surface, TS is thought to function in platelet interactions. It is also found in the extra-cellular matrix but its function here is not, as yet, undestood.

The TS gene can be induced by various transcription factors such as growth factors. For example, Marjack discovered that small amounts of PDGF produced a rapid increase in TS transcription. Cyclohexomide also induced an enormous increase in the levels of TS mRNA. Though the complete human TS gene sequence is known, no studies of the TS gene has been done. Therefore, it is thought that to understand how the TS gene is regulated, a study of the TS promoter is needed. For an initial study of the promoter, the TS promoter had to be sequenced. The promoter would then be cloned onto a bovine albumin gene and various transcription factors would be introduced to determine which factors actually induce transcription. Then an analysis would be done to see exactly where the various transcription factors affect the promoter. Finally, the effect of these factors on the TS promoter could be compared to other promoters of other genes to find similarities in the mechanism of the various promoters. Thus, the project assigned to me was to sequence a 3 kb fragment of the TS promoter upstream from an already sequenced 24kb pair promoter strand.

The DNA cosmid library obtained from another lab was cut with various restriction enzymes and fragments were produced, identified as digests. These were electrophoresed on an agarose minigel in which the digests would move according to molecular weights with the smallest pieces moving furthest and the largest moving least. A southern blot was then done in which the digests were transferred from the minigel to nitrocellulose, and a ^{32}P radioactive probe was added corresponding to the furthest upstream base pairs of the previously sequenced promoter region. Using photographic film, a radioautogram of the detected fragments from the nitrocellulose was made. By comparison with the molecular weight standards, the proper 3 kb fragment was determined to be a digest cut by the Hind 3 restriction enzyme.

†Salil Parikh is a senior chemistry major from Memphis, Tennessee.

Table 1
DNA Cosmid

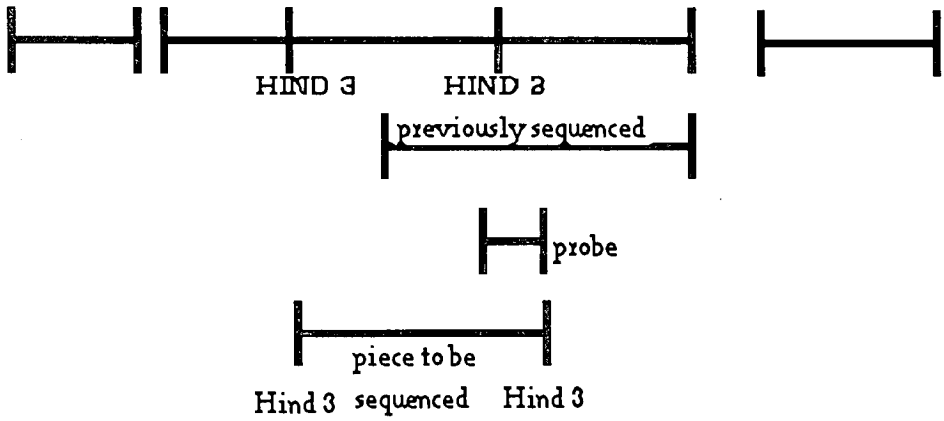

Now that the 3 kb piece was isolate, multiple copies of this fragment were needed for sequencing. To accomplish this, a plasmid was used called pBS M13^{+} which also contained a Hind 3 site. The plasmid was opened up with a Hind 3 restriction enzyme, and 3 kb piece to be sequenced (insert), was inserted into the opened-up plasmid vector. The vector and insert were attached together using a ligase to form a new plasmid containing the 3 kb fragment to be sequenced. The new plasmid was then transfected into *E. Coli* and allowed to multiply in a broth. The following table illustrates the insertion process.

Table 2

Insertion Process

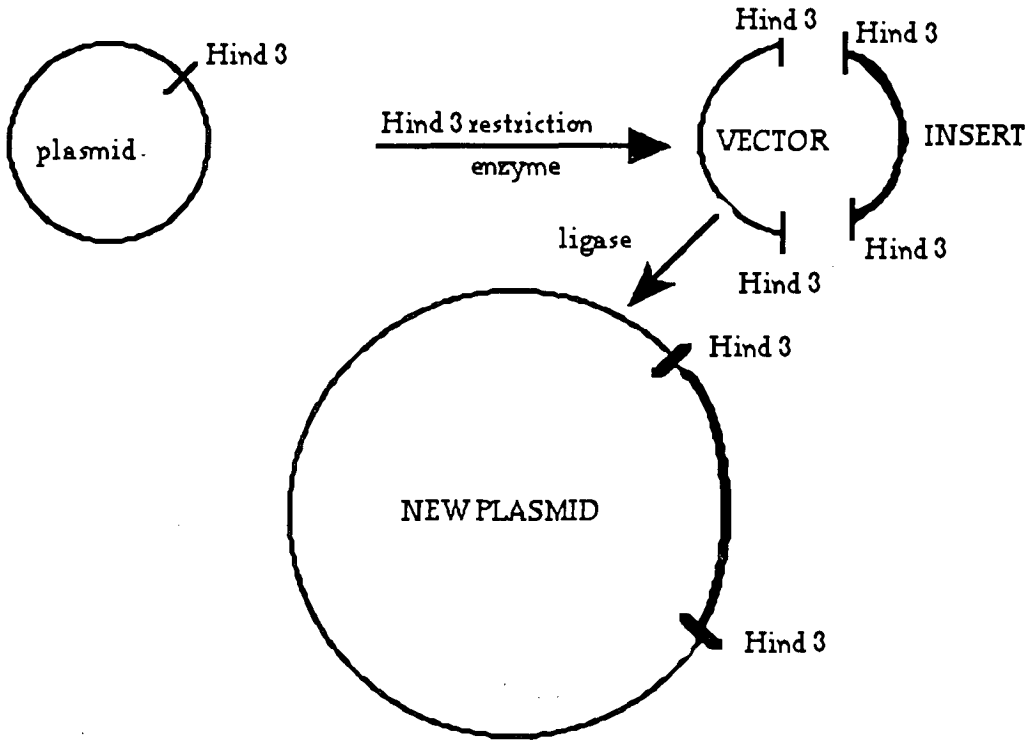

For sequencing, a primer is added to the Hind 3 site and only the first 300 bases can be sequenced after which the sequencing is indistinguisable. Therefore, bases that were further away than 300 bases from the primer had to be brought closer to the primer in order to be sequenced. Thus, an exonuclease 3 enzyme was used to cut bases close to the primer and a ligase was utilized to attach the plasmid together so that the bases that were once very far away from the primer were now close enough to be sequenced.

Table 3

Exonuclease Process

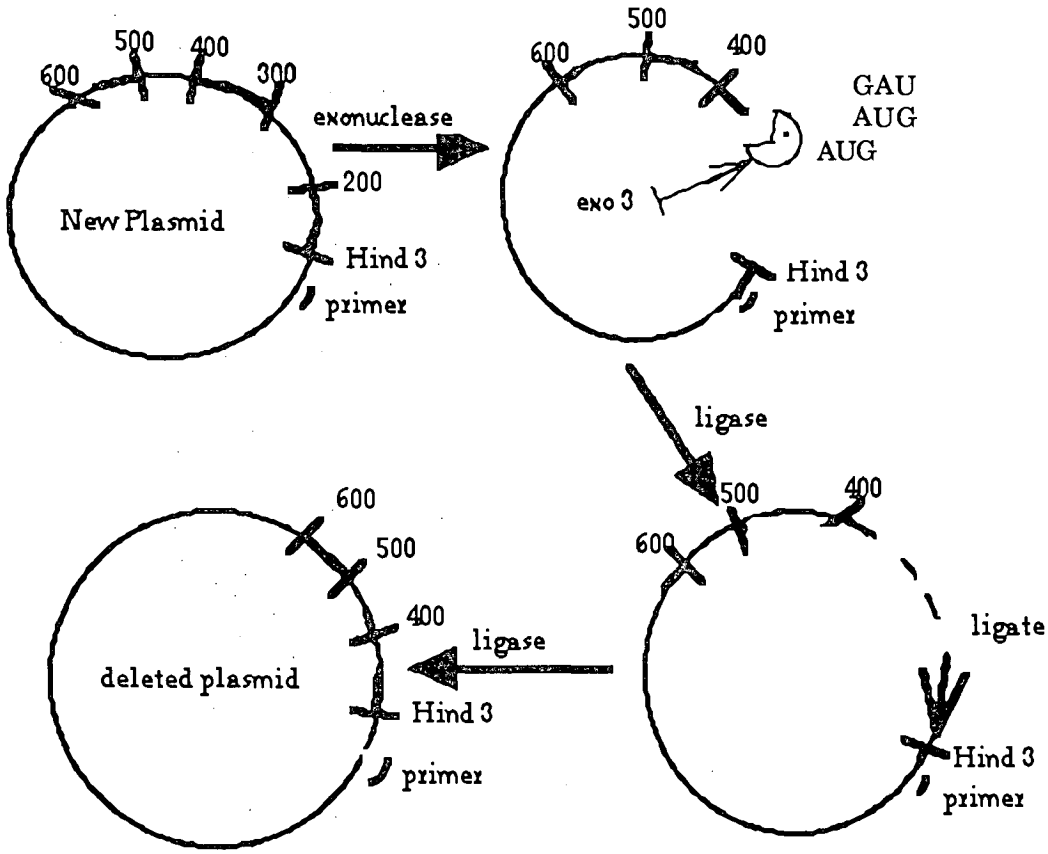

These new plasmids were again transfected into E. coli and allowed to multiply. Because a single stranded DNA was needed for sequencing, the bacteria were infected with a virus, otherwise known as helper phage, which made a single strand copy of the double strand DNA plasmid, containing the 3 kb insert to be sequenced. E. coli was then lysed, releasing the helper phage. The phage protein was then dissolved, and the single stranded (ss) plasmid was then obtained and purified.

The Sanger Dideoxy method was used to sequence the plasmid now identifed as a template. In four test tubes, the 4 dNTP's (dATP, dGTP, dTTP and radioactive dCTP) were added. However, each test tube also contains one of 4 dideoxybases, either dideoxy A, dideoxy C, dideoxy G, or dideoxy T. The ssDNA template was pipetted into all 4 tubes and a DNA polymerase was then added which formed a complimentary DNA strand, using the 4 dNTP's. When a dideoxybase was inserted in the growing DNA chair, the strand ceases to grow because of the inability of the polymerase to form a phophodiester bond with an dideoxynucleotide. The DNA strands created in the 4 test tubes were then electrophoresed on a polyacrylamide gel and, the gel was exposed to a photographic film. The sequence of bases were then read off the photographic film. For more information, see Stryer's *Biochemistry*. The following table list the 1600 bases which were sequenced.

Results

Table 4

Bases Sequenced

AGCAGGGATC	CTGTAGCAGG	AAGCACAAGA	GCCGAGGGTC	AGAGATCAGC	TAGGCAGGGA	60
GGGACGGTGC	GCAGAAACGG	GGCTGGGCAT	GGGGACAGGG	CCGGGACCAT	CCCTCTTTGA	120
CCCCGCGTTT	GCTGAAATGA	AGGACAACAG	GATTACTTTC	CAGAGAGCAT	GAGAGAGAGA	180
GAGAGAGAGA	GAGAGAGAGG	TGGAGGAAAG	AGATGCTGGT	TTTAAAGTGT	GGGGGGCGCA	240
AGACCAACAA	TTTGGGGGCT	TTTGGGAAGT	CGAAGGTGAG	CAAGATCAGG	AACTGTAGTT	300
TGGGGTTGCA	GGGAGGGCAG	GGGAAGTACA	GACTCTTCCC	TGGAGTGCTG	ATACAAAGGC	360
TTAAGGAGGA	CTTCAGAGAG	TAAGGAAATC	TTGGGGTGTC	CTGATGAGTT	GGTTTGTGAA	420
CCTCAAGGCT	GGAGAGGATG	GCTCTGGAGC	CTTGCCCTGA	AGAGTCCTCC	AGCGGCTGAG	480
AGGAGCGGGC	TGGGGTAGGC	GAGCGGGGAG	AGTGTAGGTT	CCGGGGTCCA	CCAGAGGGAC	540
TGAAGCCTCA	GCGCTCCAGG	TGGATGTCCC	GGGCAGCTTT	GGTCCTCGGC	GGCCGCCGGG	600
GGCGACTTAC	CTGTGTGTAC	CGGAGCGCGG	CGGCCGGGAG	CGGTGGCGAG	GGCGGCGAGG	660
GCTGGAGGGG	CGCGGGGAAT	GCCTGTGCGT	CCGGAGTAGA	GGTTGCTCCT	GGAGAGCGAC	720
AGGAGCCCTG	AACTCGCAGG	CCAGCTCGGG	CGCAGCGGCT	GGCAAGGCGG	AGGAGCCGCG	780
CGCTTTTAAA	GGGGCGCTCG	CATTCCTGGG	GATTCCTCCG	GCCAATGGGC	GGCGGCCGGG	840
CAGGAAGCGG	GAGGTGGGGG	CCAGTCTGGG	CTCCTCTCTC	CGCCCCCCGC	TGCCTGGCGC	900
GCAACTTTCC	AGCTAGAAAG	TGAAGGGGGC	GGGGGTCGGG	GCTTGGGAGC	ACTAGAACTT	960
CTCAGAAAAG	TCGGTGCCG	CCCACGCAGC	CTTGGCGCGC	ACGGGCTCGG	CGCTCGTACT	1020
CTTGCGCCAC	GCGGGCTCGG	GGTGATCAGC	AAGCATCCCG	AAAAGGGACG	GGGCTGGGGA	1080
GACCACCTAG	GAGGGCCCGC	GGGGTGGCGC	AGGGGCTTTC	GGGCGAGCTG	ATCTCCCGGA	1140
ATGCCTGGTT	GATGGCGAGA	GGTGGATACT	AGAGACTGGG	CCCGTTTTGT	AAAAAGAAAA	1200
ATGGGCCGAC	GGGGCGCAGG	GGACACCAAG	AGAGCCATTC	GTTAAAGTAC	CTGCCCCTCG	1260
GGCCCTCGCT	GACTCTCCTC	CACCGTCCCC	GTGGGGTGAG	GACACGCGTC	CCCCGAGCGC	1320
CTGTCCTGAG	CTGGCCCCAC	GCCCGCCCCG	GAGGGAGGTG	AGCGCGGCGT	CGGCGGGGCC	1380
GGCAGGTTGG	TGCGCCGCGT	TCGCCTTCGC	TGCCTTCGGG	CCCTTTCCTG	CCGCGGCTGC	1440
CAGGGGGCCC	ACAGAGACGC	CTCTCCCGCT	GCCGCGGCGC	TCCCTCGGCC	GGCCGCTTGG	1500

Conclusion

In future research, a transcription factor will be added and the promoter will be exonucleased base by base starting from the upstream end of the promoter to determine at exactly what sequence of bases the transcription factor acts on. This sequence of bases will then be compared to other similar sequences of bases in other promoters to determine if the promoters have similar mechanisms of function.

Literature Cited

Donoviel, Dorit, Paul Framson, Charles Elridge, Michael Cooke, Senrtaro Kobayashi, and Paul Bornstein. 1988. Structural Analysis and Expresseion of the Human Thrombospondin Gene Promoter. Personal Communication.

Stryer, Lubert. 1988. *Biochemistry*. New York: W. H. Freeman & Co. p. 117-143.

A Word with...Professor Stauffer

by Barbara Mulach

Many students at Rhodes College have had the opportunity of learning the basics of Physics from a very talented professor, Frederic Stauffer, but few students know of the interesting tales that he has to tell about his experiences over the years. I learned many facts, and heard several interesting stories in the short time I spent with Professor Stauffer, which made me realize why he is such a special member of our faculty and family here at Rhodes.

Professor Stauffer grew up a Pennsylvania Dutchman, being raised in a small town near Allentown. He left home at the age of 17 to become a radio operator in the Merchant Marine. After three years he left this position to serve in the U.S. Army, stationed much of this time overseas in Kassel, Germany and Linz, Austria, the latter service working in Military Intelligence. An interesting twist to this story is that he was the only official draft dodger of Montgomery, Pennsylvania, receiving his final notice two days after the assigned date in Naples, Italy. His ship sailed the next day for the invasion of Southern France. (What a way to dodge the army.) In 1945, his ship was involved in a collision at sea which cut another ship in half. Prof. Stauffer was later hospitalized in Kassel, Germany. There he met an Army nurse named Helen who later became his wife. Another interesting tidbit--He once proposed to a niece of the late Czar of Russia, just to have some interesting stories to tell his grandchildren. (He never called her for her reply.)

Though unsure of his plans when starting college, Professor Stauffer followed his interests in Physics and Mathematics, obtaining his B.S.(1951) and M.S.(1952) in Physics from Bucknell University. He then studied further with the famous Dr. John Strong at The Johns Hopkins University from 1957-1963. His topics of specialty included Structure of Line Spectra, Derivative Spectroscopy, and Planetary Atmospheres.

In 1954, he began his teaching career, first at his alma mater, Bucknell University, and several years later here at Rhodes College (then Southwestern at Memphis) starting in 1964.

While at Rhodes, Professor Stauffer's interest in baseball led him to become the assistant coach of the Rhodes baseball team from 1968 to 1973 and head coach from 1973 to 1977, his last team convincing the Board of Trustees to name the field in his honor, now known as Stauffer Field. Other activities include his recent work with amateur radio, communicating with other radio operators around the world. He is also licensed to provide emergency communications in emergency tests and natural disasters as a public service. He plays at golf, strongly emphasizing the fact that it is not one of his great talents. As for future interests, Professsor Stauffer is considering an invitation to study ozone recombination rates with Dr. John Strong at the Astronomy Research Facility of the University of Massachusetts at the beginning of next year. This work requires a great deal of strategical planning as well as actual experimentation, which would provide a challenging as well as alluring opportunity for study.

Speaking with Professor Stauffer, I got the genuine impression that he enjoys his work with students as well as his continuous research and activities. He has contributed a great deal to the development of Rhodes and its many students over the last 25 years. This is probably the reason why he is so loved and respected among Rhodes students who have had the opportunity to work with him in the many years he has served Rhodes College.

Professor Frederic Stauffer is Associate Professor of Physics at Rhodes College. He is married and has 4 sons, 8 grandchildren.